A Novel 3D Model-Based Petroleum Resource Estimate of the Qaidam Basin in Northwest China and Implications for the Future of China's Energy Economy

A thesis presented by

Josh Grossman

to

The Department of Earth and Planetary Sciences

and

The Department of East Asian Studies

in partial fulfillment of the requirements

for a degree with honors

of Bachelor of Arts

Harvard College

Cambridge, Massachusetts

Abstract

The Qaidam Basin is one of China's seven largest inland petroliferous basins and has been a center of the nation's petroleum production since the 1950s. The basin is located in Northwestern China and contains several petroleum systems. Three of these systems account for the vast majority of the total basin resources: The Quaternary petroleum system in the northeast of the basin, the Paleogene petroleum system in the northwest of the basin, and the Jurassic petroleum system to the southern basin. This study models these three petroleum systems in a 3-dimesional evolutionary model built in Schlumberger's state-of-the-art Petrel 2019 and PetroMOD 2019 software. This model incorporates geologic, well, and seismic reflection data that constrains the 3D subsurface geometry, lithologic facies, hydrocarbon chemical properties, heat flow, hydrogen index, and total organic carbon content. The hydrocarbon resource estimates (7.69 gigatons of oil and natural gas) produced from this model are substantially higher (from 25 to >200%) than previously published results. Specifically, this study confirms the largest prior estimates of the basin's natural gas resources and suggests an ≈ 40% greater total oil resource than previous estimates. The spatial distribution of petroleum accumulations generated by the model indicates the possibility of increased gas potential in the northwestern Mangya depression and greater potential for oil extraction in the southern Qaidam Basin. Natural gas produced from the basin will almost certainly be consumed domestically given China's ever-growing demand for natural gas, which is driven in part by government policies encouraging citizens and towns to switch from coal-powered heating systems to natural gas-powered heating systems in an attempt to curb pollution. However, the future of the basin's oil resources is much less clear. As transportation costs remain high given the basin's remote location, it is possible some of the oil resources in Qaidam will eventually become exports along China's Belt and Road Initiative or go

to plastics manufacturing in the area. This model's results are significant in helping build a greater understanding of the relative contribution of each distinct petroleum system to the total resources present within the Qaidam basin as well as in helping guide future exploration toward several target areas.

Table of Contents

List of Figures

Acknowledgements

This thesis process has been arduous and rewarding in equal measure. From the beginning of junior spring to now in my senior spring this thesis has transformed me from someone who just thought energy systems were cool to a geological modeler and researcher. This transformation and this research would not have been possible without a great many people.

I would first like to thank my Earth and Planetary Science advisor, Professor John Shaw, who guided me to this project when I was but a bright eyed and bushy tailed junior looking to study an energy system somewhere in China. I would next like to thank the newly minted Dr. Yanpeng Sun, whom I worked with closely during my junior spring and whom I had the tremendous privilege of traveling with to present our results to PetroChina's office in Dunhuang. I would also like to thank Dr. Andreas Plesch, whose help was truly invaluable in building the PetroMOD model and served as a constant source of good advice. I would like to thank Franklin Wolfe who was my compatriot in frustration with Petrel and a great help. I would like to thank Jessica Don and Sage for providing insight and inspiration. I would like to thank Benjamin Chauvin for providing general wisdom. I would like to thank Esther James and Annika Quick for their dedication to the thesis writing process and their constant support. I would like to thank Chenoweth Moffat for her constant support, encouragement, and supply of ginger chews. I would also like to thank Jerry Mitrovica, who taught the very first EPS class I ever took and inspired me to concentrate in the Earth Sciences.

I would like to thank my East Asian studies advisor, Professor Michael McElroy for his insight into the implications of my results, and for his guiding wisdom in understanding the greater energy economy at play. I would like to thank Shaojie Song who advised me and kept me on track. I would also like to thank Professor Ryuichi Abe for believing in me and supporting

this project when I first explained to him my plan to combine Earth and planetary sciences and East Asian studies for a joint thesis.

I would like to thank my many Chinese language teachers over the years. From Zhang Laoshi and Ms. Shorter at Brookline High School to Zhang Laoshi, Wei Laoshi, Zhao Laoshi, and Fu Laoshi at Harvard. Their patience and instructing acumen gave me the language skills I needed to understand the all-mandarin software, GeoMAP, and read several articles only available in Mandarin, which proved extremely helpful.

I would like to thank our friends at PetroChina, particularly Dr. Guan Shuwei, for their help with and support for this study. None of the research would have been possible without the subsurface contour maps they shared and for those I am extremely grateful. I am also especially grateful to PetroChina for their inviting Dr. Sun and myself to present at their offices in Dunhuang during the summer of 2019, it was quite the honor to travel there and learn from the people who are doing the actual work in the Qaidam Basin.

I would like to thank Schlumberger for their generous grant, valued at $11.5 million USD, for software licenses for Petrel 2019 and PetroMOD 2019. These software applications were essential to the building of the model used in this study and I am grateful for their use. I would also like to thank Tayo at Schlumberger PetroMOD support for his invaluable help with troubleshooting several key technical issues.

I would like to thank the other EPS thesis writers for their camaraderie and compassion as we struggled together. I would like to thank my friends and family for their tireless support. And finally, I would like to thank you, whoever you are, for taking the time to read this thesis, it means quite a lot to me.

Introduction

1.1 Motivation for this Research

This thesis seeks to provide a novel, model-based estimate of the total hydrocarbon resources accumulated in the Qaidam Basin in Northwest China. The Qaidam Basin is a critically important basin in China's energy economy, particularly due to its high natural gas production capacity. Natural gas is a key resource in China's pollution reduction strategy and a major energy security concern for the nation. This thesis will subsequently explore the implications of the geological resource estimate provided.

1.2 The Qaidam Basin

Located in Northwestern China, the Qaidam Basin is a tremendously important inland basin in the context of China's energy economy, largely owing to its recoverable oil and natural gas resources. Located on the northern margin of the Tibetan Plateau and with an average elevation of 2800 meters, the Qaidam basin is China's highest petroliferous basin. Figure 1.1 shows the location and the topography of the basin in this context.

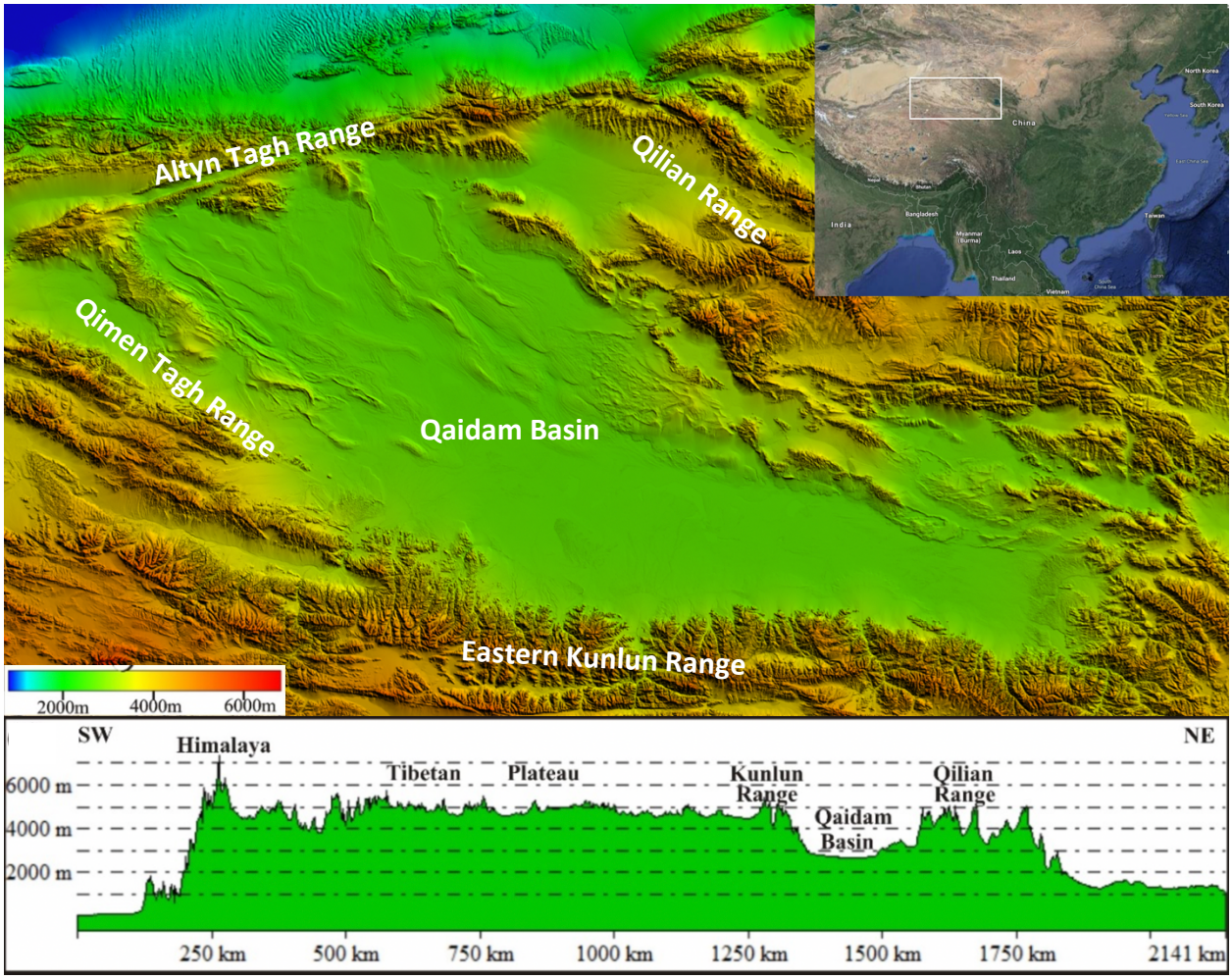

Figure 1.1a Index map of the Qaidam Basin and 1.1b Elevation profile of the Qaidam Basin (Sun, 2019).

The basin has an area of 250,000 square kilometers, and is bordered by the Kunlun, Altun Tagh, and Qilian mountain belts. The name Qaidam is Mongolian in origin and means "salt pond." The basin's name in mandarin is Chaidamu (柴达木). The Qaidam basin lies between the provinces of Xinjiang, Qinghai, and Gansu (China National Petroleum Corporation, n.d.). While Qinghai and Gansu are fairly typical provinces administratively speaking within the People's Republic of China, Xinjiang has a highly complicated and contentious political history and is considered to be an 'Autonomous Region' by the national government. Since the 1950s, the Qaidam basin has been noted as a considerable source of

Chinese oil and gas reserves. Commercial exploration of the Qaidam Basin began as early as 1954 (Gu Shusong & Di Hengshu, 1989), and ever since the basin has been a significant source of hydrocarbon production in China. The Basin is also unique in that it possesses coal beds as well as recoverable oil, thermogenic natural gas, and biogenic natural gas. Given the Qaidam basin's location on the Tibetan Plateau, there are many interesting aspects to the geology of the region. The basin's formation and structure are related to the large-scale tectonism caused by the collision of the Eurasian continental crust with the Indian subcontinent (Molnar & Tapponnier, 1977). The Basin's formation is theorized to have been spurred by the need to accommodate crustal buckling as well as lateral movement of the Eurasian continental caused by the collision with the Indian subcontinent (Q. Wang & Coward, 1990). Ultimately, all of the geological conditions of the basin's formation have resulted in a hydrocarbon rich environment with multiple formations conducive to commercial production of oil and gas. This thesis comes at a time of increasing Chinese energy usage and increasing Chinese global trade presence due to the Belt and Road Initiative. This thesis provides the first independent, comprehensive three-dimensional evolutionary basin model for Qaidam, and will explores the implications of the resource estimates provided by the model.

1.3 Qaidam's Current Place in China's Energy Economy

The Qaidam basin is currently one of China's highest-producing petroliferous basins. The Qinghai oilfield is the largest field in the basin producing 2 million tons of oil (~14.6 million barrels) and 8.55 billion cubic meters (~300 billion cubic feet) of natural gas annually. The Gasikule area within Qinghai produces 1 million tons of oil annually. The area also has substantial petroleum refining and transport systems including the million-ton-per-year Golmud refinery and the 436-kilometer Huatugou-Golmud oil pipeline. Six natural gas pipelines and the Huatugou-Golmud pipeline make for a total of 3,159 kilometers of pipe in the basin. The basin's total petroleum transport infrastructure can accommodate 3 million tons of oil and 10.7 billion cubic meters of natural gas each year.

In 2016 China consumed 208 billion cubic meters (7,345 billion cubic feet) of natural gas ("National Bureau of Statistics," 2016). As such, in 2016 the Qaidam basin produced 5.14% of China's natural gas consumption (China National Petroleum Corporation, n.d.). In 2016, Fu et al. posited a proven ratio of gas in the basin of 10.8% (S. Fu, 2016). The proven ratio, commonly used by Chinese petroleum geologists, represents a ratio of proven hydrocarbon reserves to total geological resources. It is never expected that all resources can be developed (i.e., the proven ratio reaches 100%). Rather, lower values (≈ <30%) imply that the basin has significant remaining exploration potential, while higher values (≈ >30%) suggest that much of the basin's resources have been discovered. The 10.8% proven ratio provided by Fu et al. (2016) indicates that the basin is in an early phase of development with respect to natural gas. Fu et al. (2016) also identifies a 21% proven oil ratio, which would indicate that the basin has seen more relative development of its oil fields, which is consistent with historical trends for basin development (S. Fu, 2016). This thesis will explore a new,

comprehensive model-based framework with which to establish estimates of oil and gas generation, expulsion, and accumulation in the Qaidam basin.

1.4 China's Natural Gas Supply

China's natural gas demand has been rising for the past half century, with sharp yearly increases in demand for natural gas every year since 2000. Natural gas now takes up a greater percentage of China's overall energy mix than ever before ("National Bureau of Statistics," 2016). Figure 1.2 illustrates Chinese natural gas consumption and production over time.

Chinese Consumption and Production of Natural Gas 2005 - 2015

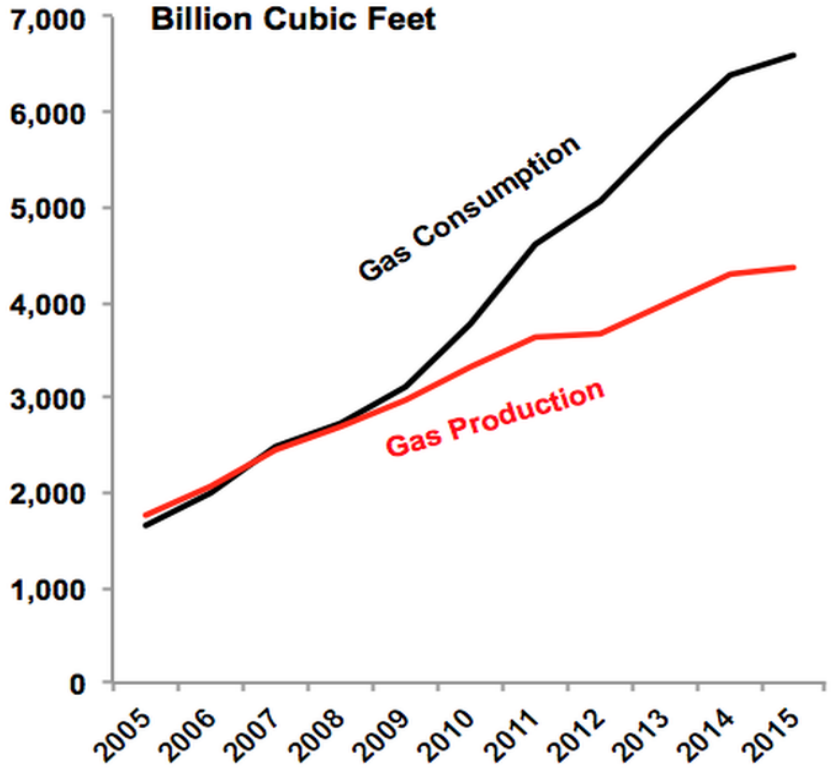

Figure 1.2 Chinese consumption and production of natural gas 2005-2015 (Clemente, 2016)

The Qaidam basin, producing 10.7 billion cubic meters (377.5 billion cubic feet) of natural gas per year, is one of China's most prolific domestic gas-producing basins. Even though domestic natural gas production has more than doubled in the past ten years, it still

cannot keep pace with demand. The sharp increase in Chinese natural gas demand is due in part to government policies encouraging citizens and towns to switch from coal-powered heating systems to natural gas-powered heating systems in an attempt to curb pollution (Guo et al., 2018). Pollution caused by coal use for residential heating is a substantial contributor to overall smog, particularly in Northern China (Clemente, 2016). These so called "coal to gas," policies have had mixed results. While these policies have reduced pollution substantially, they also led to severe natural gas shortages throughout the 2017-2018 winter, leaving many without the ability to heat their homes, office buildings, or schools (Guo et al., 2018). While the government has been more vigilant in ensuring security of natural gas supplies since the gas shortages, natural gas supply remains a crucial concern of energy security in China. It is in this urgent context that this thesis examines the natural gas and oil resources of the Qaidam basin.

1.5 The Belt and Road Initiative

A major contemporary Chinese foreign policy initiative, the One Belt One Road (一带一路) policy is important context to provide for understanding potential upside of continued hydrocarbon exploitation in the Qaidam basin. The policy, known in English since 2016 as the Belt and Road Initiative (BRI), is a global development and investment strategy aimed at growing Chinese influence around the world and growing soft power, nonmilitary power such as economic or cultural influence (Sorin-George & Cătălin, 2018). Figure 1.3 provides a graphic representation of the BRI's expansive reach along with lines representing current and planned oil and gas pipelines.

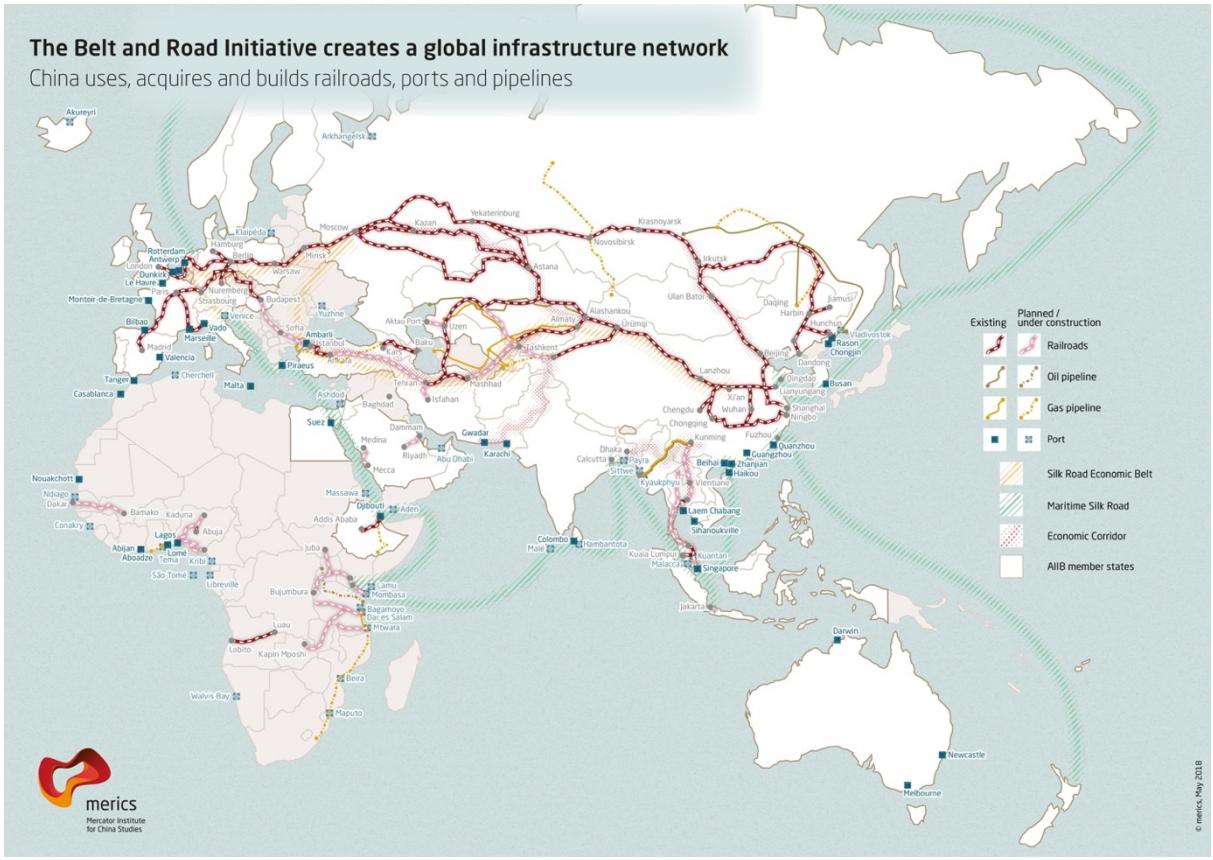

Figure 1.3 Map of Belt and Road Initiative alongside existing and planned oil and gas pipelines (Eder, 2018)

The BRI takes its name from the ancient Chinese silk road, a legendary trade route that stretched for thousands of miles, connecting Asia, Europe, and Africa. While the belt refers to land trade routes, the road aspect of the BRI refers to maritime trade routes. The modern BRI includes infrastructure investments in over 70 countries throughout Asia, Africa, and Europe, with over $90bn USD committed via the BRI fund and the Asian Infrastructure Investment Bank to go toward BRI infrastructure projects. The policy has many aims, among them are expanding Chinese global influence, increasing the use of the Chinese national currency (RMB) in large transactions, securing reliable supplies of raw materials needed for manufacturing or energy, developing relationships with potential markets for Chinese products, and improving infrastructure to aid in and facilitate the transport of products, with particular attention paid to energy resources (Sorin-George & Cătălin, 2018).

China has received some international criticism for the Belt and Road Initiative on the grounds that many of its aims are neo-colonialist in nature. This is particularly important as pertains to environmental equity. While China is trying to shift its energy mix away from coal and towards natural gas, the BRI's infrastructure plans include building coal power plants throughout Africa (Ullman, 2019). As such it is difficult to overstate the importance of the Belt and Road Initiative in determining China's energy future, not only the future of China's energy consumption but also the future of China's domestic energy production, exports and imports, as well as China's future energy mix.

Hydrocarbon Terminology and Theory

2.1 Terminology and Units

To understand model results in context, it is essential to first establish the terminology of petroleum systems and of the associated large-scale oil and natural gas accumulations. Oil is typically reported in either billion barrels (BBBO) as a measure of volume or in gigatons (10^9 metric tons) as a measure of mass. Traditionally, US-based literature uses barrels while Chinese geoscientists prefer to use gigatons or other metric units. Natural gas is reported in either billion cubic feet (BCFG), trillion cubic feet (TCFG), or billion cubic meters (BCMG). Similar to oil, US-based researchers and companies publish numbers in imperial TCFG while Chinese sources generally use metric BCMG.

The gas to oil ratio (GOR) is a theoretically unitless ratio which measures the ratio of gas to oil for a particular well, reservoir, or basin. In practice, however, there are units implied since the different measures of oil and natural gas resources must be specified for their ratio to be properly comparable. In this thesis as in much of the established literature, GOR will be calculated in cubic feet of gas to barrels of oil.

In hydrocarbon terminology there is an essential difference in meaning between a geological resource and a reserve. Resources are estimated by geologists with varying degrees of accuracy and represent an upper bound on the mass and volume of hydrocarbons present in a petroleum system or given area. This thesis offers novel, model-based estimates for the Qaidam basin's total geological resources. Oil resources are also sometimes referred to original oil generated in place (OOGIP). A reserve, on the other hand, is the quantity of hydrocarbons that has been proven to an extent by well measurements and which are

extractable under current economic conditions (Besson et al., 2003). Figure 2.1 is a McKelvey diagram from Our World in Data which explains the relationship between the two visually (Ritchie & Roser, 2020).

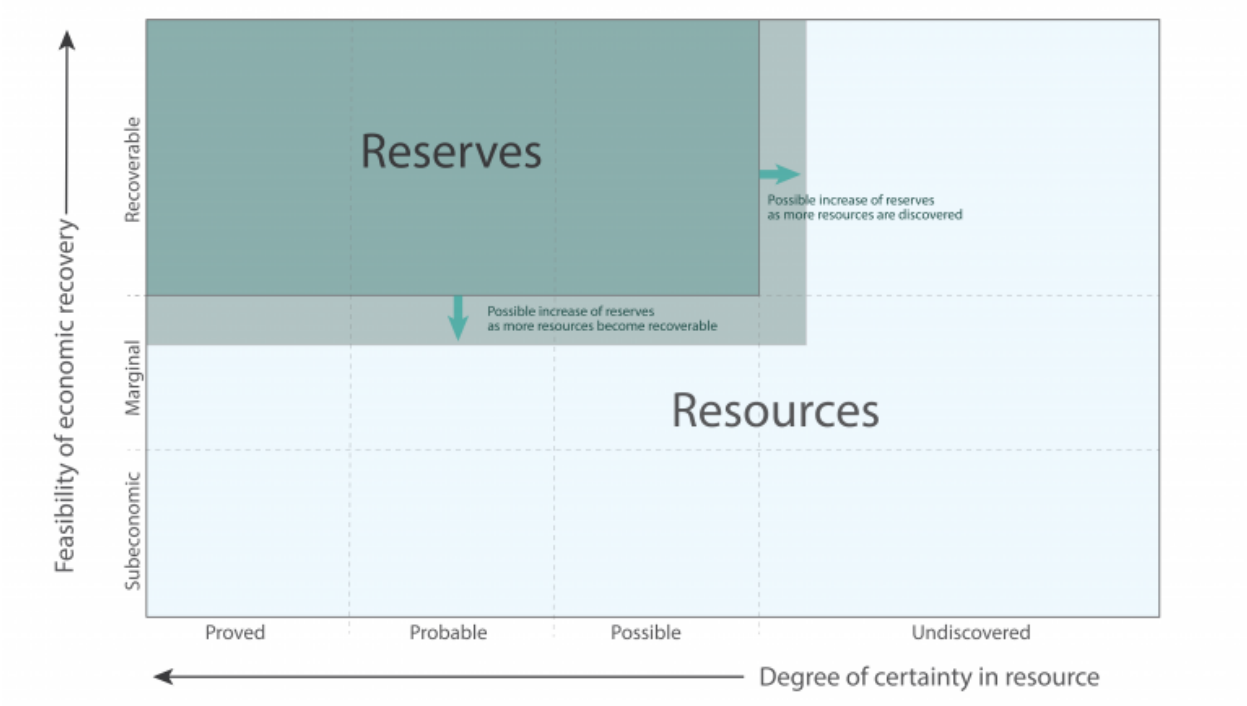

Figure 2.1 McKelvey Diagram depicting resource-reserve relationship (Ritchie & Roser, 2020)

2.2 Petroleum Systems

In the process of basin modeling, identifying petroleum systems and their properties is an essential initial step. A petroleum system consists of a source rock, a reservoir rock, a sealing rock, and a trap. Petroleum systems may produce either oil, natural gas, or a mixture of both, depending on their composition and other environmental factors. The source rock must have a high organic content and have been buried to a depth conducive to hydrocarbon maturity. In order to create a high-quality source rock, at the time of sedimentation not only must the sediments contain organic carbon, but they must be deposited in an anoxic environment with a high rate of sedimentation so that the organic content-rich sediments are not decomposed by detritivores. Figure 2.2 illustrates the ideal sedimentation process for a high-quality source rock.

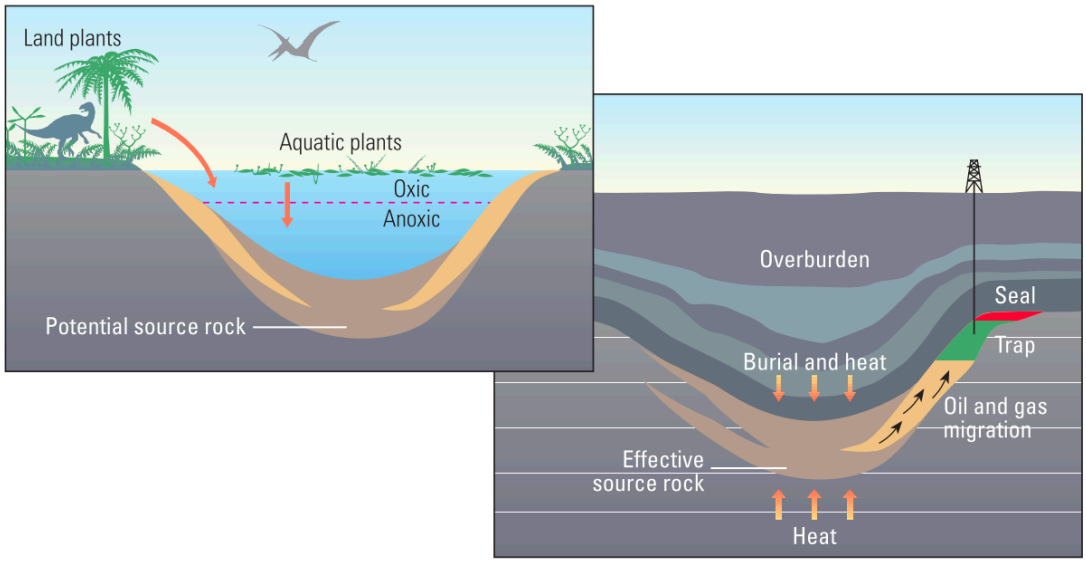

Figure 2.2 Petroleum system formation (Al-Hajeri & Saeed, 2009). The first panel illustrates the deposition of organic material in a potential petroleum producing environment while the second panel depicts the maturation and trapping of petroleum underneath the subsurface

Once the source rock has been buried, it must reach a certain burial depth such that the hydrocarbons are effectively thermally matured into oil and gas. Once the hydrocarbons are matured, a fraction of them will be expulsed from the source rock and more upwards into the overlying stratigraphic layers. For the proper development of a petroleum system the hydrocarbons must be able to migrate into a reservoir rock once they are expulsed; high-quality reservoir rocks have high porosities and permeabilities, allowing hydrocarbons to be stored within. Once the hydrocarbons have entered a reservoir rock, they must somehow be kept there in order for an exploitable petroleum system to develop. Due to their buoyancy, hydrocarbons naturally migrate upwards over geologic time, and therefore the next essential element of a petroleum system is a sealing rock. Evaporites and shales often make good sealing rocks due to their low permeabilities. Sealing rocks halt the upwards migration of hydrocarbons over time and keep them in place so that they can be drilled for and extracted. Sealing rocks prevent the vertical movement of hydrocarbons, but hydrocarbons will still tend to migrate horizontally if there is a pressure gradient. Thus, the final element necessary for the production of an exploitable accumulation of hydrocarbons is a trap. Traps come in many forms; figure 2.3 illustrates some of the more common types of traps such as stratigraphic traps, fault sealed traps, and fold traps.

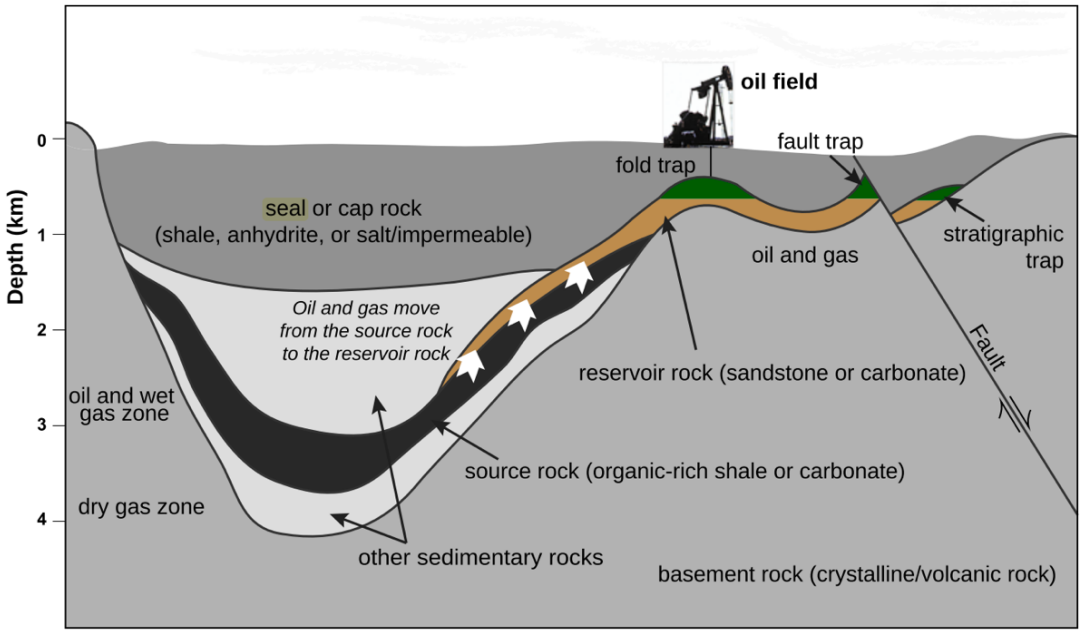

Figure 2.3 Petroleum trap structures (Shaw, 2018)

Geologic Setting

3.1 Tectonics Surrounding the Basin

The Qaidam basin is located on the Tibetan plateau in Western China. It has been theorized that the Paleozoic basement of the basin was formed as a Variscan fold belt, one that was approximately contemporaneous with Euramerica and Gondwana colliding and forming Pangea between the late Devonian and early Permian (Gu Shusong & Di Hengshu, 1989). However, the most locally relevant macro-scale tectonics to the Qaidam basin are those related to the collision of the Indian and Eurasian plates during the Eocene (Meng & Fang, 2008). Figure 3.1 presents a geological map of the basin.

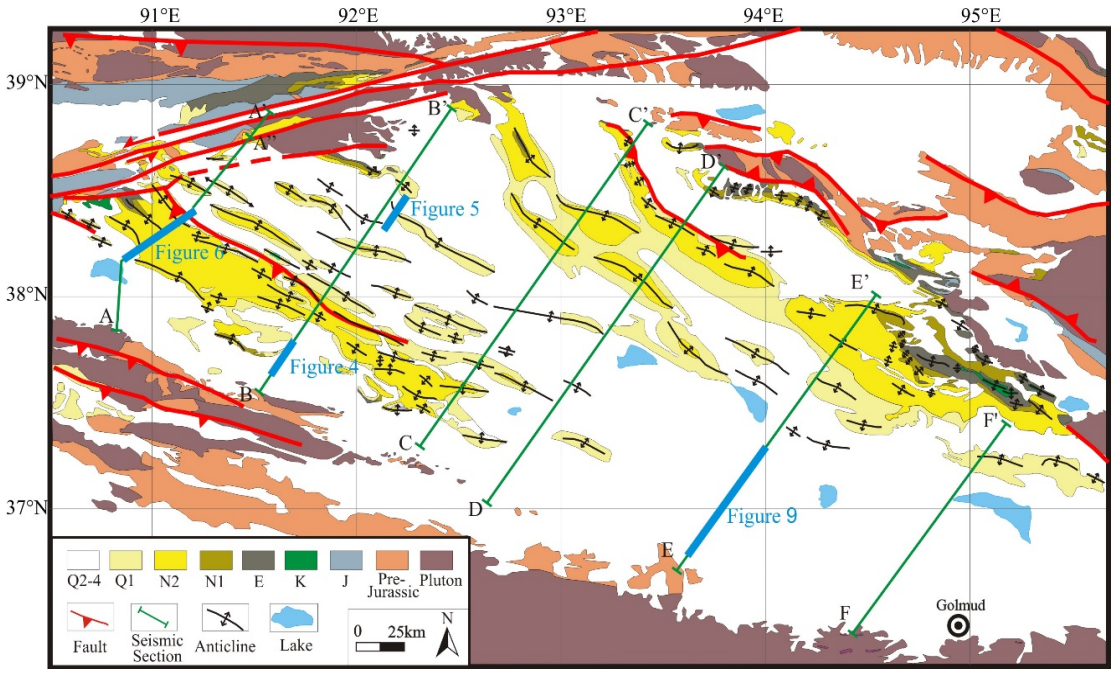

Figure 3.1 Geological map of the Qaidam basin with major faults and anticlines (Sun, 2019). The long red fault to the north of the basin is the Altyn Tagh fault.

The basin is bounded to the north by the Altyn Tagh fault, a major strike-slip fault approximately 1600 km long that has been active since the collision of the Indian

subcontinent with the Eurasian plate. Estimates on the initiation of the Altyn Tagh fault (ATF) range from 35 million years ago to 50 million years ago (Zhuang et al., 2011). The ATF plays an important role in accommodating eastern extrusion of tectonic blocks that is driven by crustal shortening in the North-East direction caused by the collision of the Indian and Eurasian plate (Tapponnier et al., 2001), (Meade, 2007). Yue et al. (2004) argue that since the early Miocene the ATF has had a slip rate of about 10mm/yr, which was significant in accommodating crustal shortening from the Indo-Eurasian convergence (Yue et al., 2004). The Qaidam basin is bounded by the Kunlun fault to the South, and by the Qiman Tagh mountains to the West (B. Fu & Awata, 2007). To the East, the basin is bounded by the Southern Qilian mountains, which were formed by fold and thrust belt system, which also accommodates eastward extrusion of tectonic blocks along the Altyn Tagh and other fault systems (Zhuang et al., 2011). The large tectonic stresses that have been placed on the basin from the eastward collision of the India-Eurasian plate convergence have helped to create a complex series of faults and related anticlines throughout the Qaidam basin, particularly in the Northwest and Northeast parts of the basin. These structures, along with the bounding mountain belts, have provided sources of sediments that fill the basin and drive its ongoing subsidence. Figure 3.2 shows a cross section of the basin which illustrates some of this subsidence.

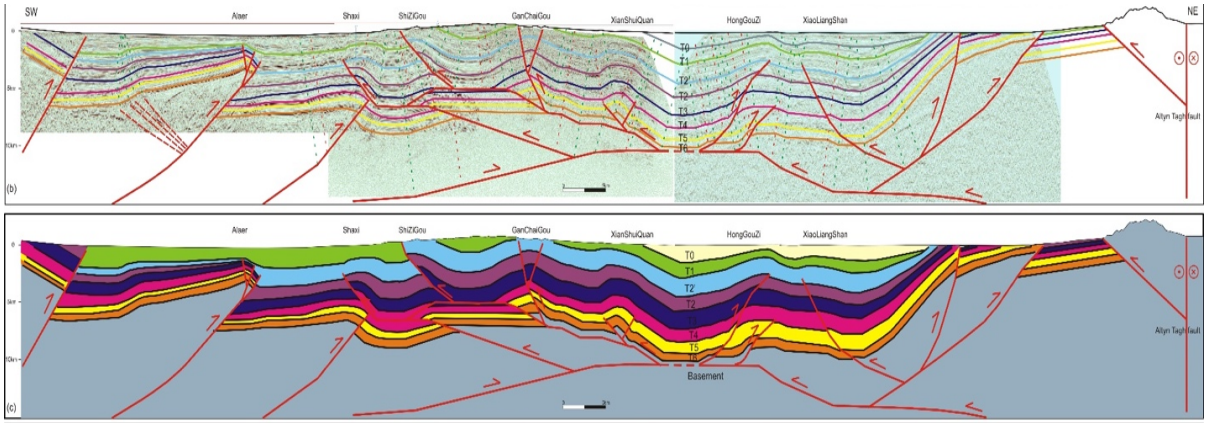

Figure 3.2 AA' Cross Section of the Qaidam Basin based on interpretation of seismic reflection profiles (Sun, 2019). Geographic location of the AA' cross-section can be found in figure 3.1 to the northwest, the AA' cross section is the line between A and A'. The top of the green section is the T0 surface, the top of the light blue section is the T1 surface, the top of the light purple section is the T2' surface, the top of the dark purple section is the T2 surface, the top of the hot pink section is the T3 surface, the top of the yellow section is the T4 surface, the top of the orange section is the T5 surface, and the top of the grey section underneath is the T6 surface. Discussion of the T# nomenclature can be found in section 3.3.

3.2 Basin Formation

Many theories abound as to the timing and mechanism of formation of the Qaidam basin. In their 1989 paper, Gu and Di argue that the Mesozoic Qaidam basin evolved in a three-step process beginning in the late Triassic (Gu Shusong & Di Hengshu, 1989). They suggest that the basin began as a foreland basin on the SW side of the Qilian mountains in the Triassic, which then subsided as a result of sediment accumulation beginning in the early Tertiary period. They then describe a third step of this process involving Eocene uplift caused by the India-Eurasia plate convergence and subsequent depocenter shift from west to east (Gu Shusong & Di Hengshu, 1989).

In their 2008 paper, Meng et al. propose that the major basin formation didn't begin until the Eocene and occurred as a result of subsidence caused by crustal shortening and subsequent buckling or flexure. They argue that contractional forces within the Eurasian plate caused the crust to buckle into a synclinal depression. Their theory is supported by the fact that the depocenter has changed very little throughout time, only exhibiting a west to east movement beginning in the Miocene. They further support their argument by providing evidence of concomitant deformation at the north and south end of the basin, which would have been deformed at the same time under a buckling model, and by proposing a mechanism for the formation of the nearby Suhai and Kumukol basins (Meng & Fang, 2008). The basin formation theory advanced by Meng et al. argues that there was likely a proto-basin present in the Mesozoic era, either formed as a moderate flexural basin or formed in an extensional setting. Figure 3.3 describes the general crustal buckling process described by Meng et al. (2008) and the associated pattern of thrusting within and along the basin margins.

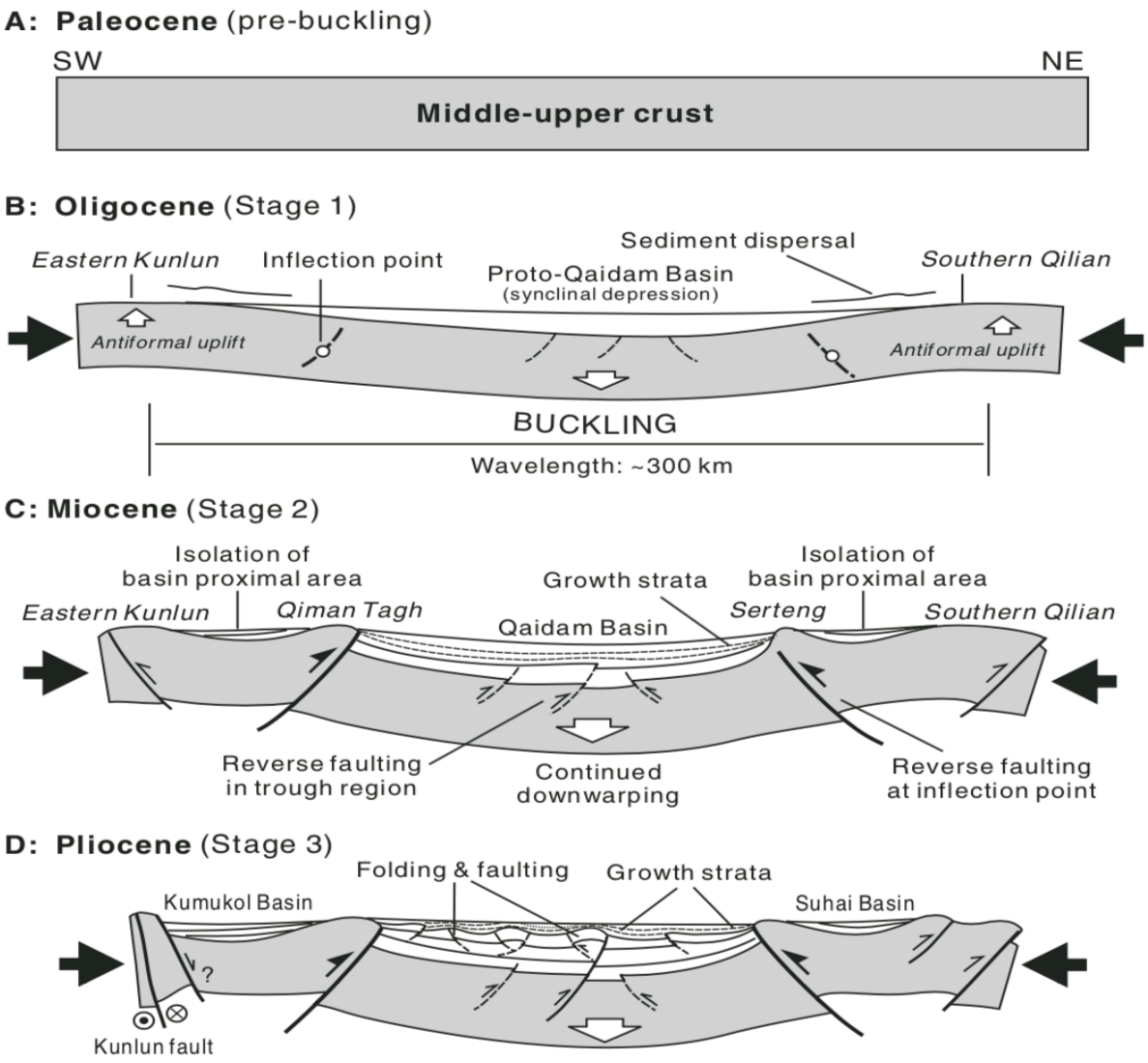

Figure 3.3 Illustration of the Crustal Buckling Hypothesis (Meng & Fang, 2008)

Although these are two distinct theories, both contain valuable insights into the current structure of the Qaidam basin. The models describe an early-formed basin that has maximum subsidence in its center. This provides an ideal paleo-environment for the deposition of potential source rocks as described by Gu and Di in (1990). The resulting Jurassic and Tertiary source rocks were described and evaluated in terms of resource

potential in (S. Fu, 2016). The Meng et al. theory provides a strong argument for the formation of reverse faults within and around the basin's edges. It is likely that some combination of the two theories is correct, perhaps Gu and Di accurately predicted the Mesozoic formation of the proto basin, but the basin's current structure is mostly due to the crustal buckling theorized by Meng et al.

3.3 Stratigraphy and Lithology of the Basin

The Qaidam basin contains formations and sediments spanning many time periods, from Precambrian to present day. Precambrian basement and Paleozoic rocks are exposed at the surface along the basin margins, and more recent Mesozoic and Cenozoic sediments and sedimentary rocks are present in the basin center. The model presented in this thesis simulates basin evolution as far back as 160 million years and includes Jurassic and Tertiary source rocks. The Jurassic source rocks are primarily shales and siltstones, many of which formed in fluvial or lacustrine settings. The primary Tertiary formations of interest which have been identified throughout the basin and some surrounding areas are the Lulehe, the Xia Ganchaigou (lower Ganchaigou), the Shang Ganchaigou (upper Ganchaigou), the Xia Youshashan (lower Youshashan), the Shang Youshashan (upper Youshashan), and the Qigequan (Zhuang et al., 2011). Figure 4 details the time of formation and theorized geological conditions surrounding each formation as well as significant, contemporary tectonic events.

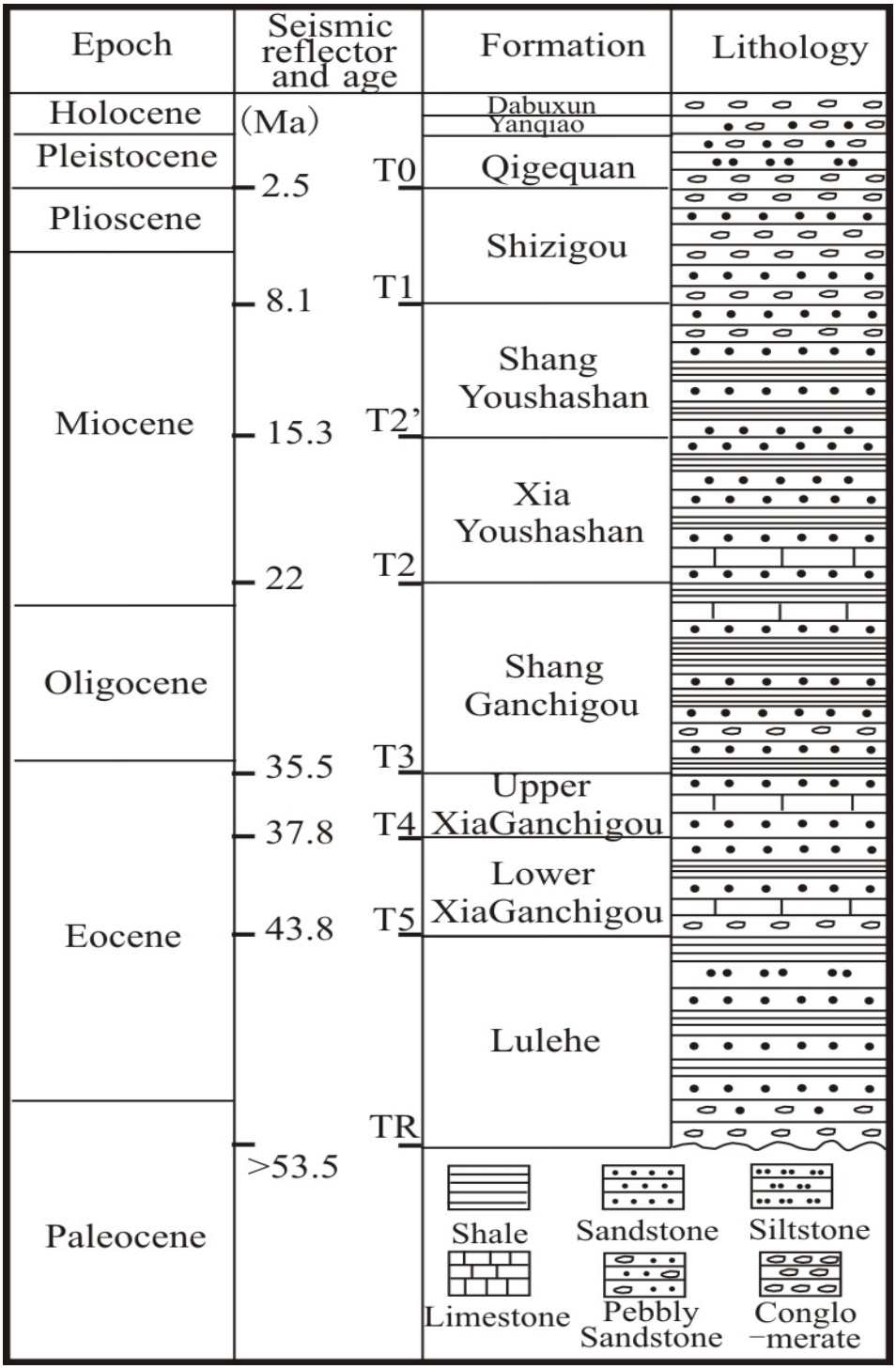

Figure 3.4 Stratigraphic column (Sun, 2019)

The T# nomenclature is used in several papers about the Qaidam basin due to its use by geologists at PetroChina. Each T-number represents the change from one formation to the next. Each T-number corresponds to a horizon, which can be created as a 3D surface from seismic reflection data. Each point on the surface is the elevation at which one formation becomes dominant over the one beneath for every XY point in the basin. The surfaces obtained from this method are incredibly valuable in basin modeling as they help constrain the size of the rock units within the context of the basin and they are the primary data source for all 3D geometrical modeling.

The early Eocene Lulehe formation includes pebble-cobble conglomerate clasts and is theorized to have formed in braided river systems. The Xia Ganchaigou from the late Eocene originated in a meandering river system and includes mudstone and sandstone beds. The Shang Ganchaigou is of lacustrine origin, and includes mudstones, and contains some thin evaporite layers. The Xia Youshashan formed in a marginal lacustrine setting and contains more sandstone than the nearby Shang Ganchaigou. The Shang Youshashan was deposited in a braided river system and contains course sandstone and conglomerates. The Shizigou formation formed in an alluvial fan environment and is similar to the Shang Youshashan formation although it has composed primarily of the pebble-cobble conglomerates (Zhuang et al., 2011). The Quaternary Qigequan is the youngest formation, deposited beginning approximately 2.5 million years ago, and is comprised of rough grained sandstone and conglomerates, likely deposited in an alluvial-fluvial system (Meng & Fang, 2008).

The history and lithology of these formations has been used extensively by Meng et al. (2008), and Zhaung et al. (2011) to understand the structural geology of the basin through time. Meng et al. (2008) uses the near-identical patterns in outcropping of these formations in

the North and South end of the basin to support their theory of crustal buckling. Zhuang et al. (2011) uses different locations along the Altyn Tagh Fault (ATF) with near-identical formation patterns to understand and bound the slip rate on the ATF.

3.4 Petroleum Systems Present Within the Basin

The vast majority of energy resources in the basin are produced from oil- and gas-bearing Jurassic and Tertiary source rocks, and the gas-bearing Quaternary source rocks. There are alluvial fan deposits, fluvial deposits, lacustrine deposits, and aeolian deposits present throughout the basin since the environmental and ecological setting of the basin has changed so dramatically over time. These strata provide the elements of the petroleum systems that we will evaluate, including the source, reservoir, and seal assemblages. This thesis studies and models three distinct petroleum systems: the Jurassic petroleum system in the North East of the basin, the Quaternary petroleum system in the Sanhu depression, and the Paleogene-Neogene petroleum system located in the Northwest of the basin. Figure 3.5 from Fu et al. (2016) illustrates the locations of these source rocks of some of the basin's major discoveries.

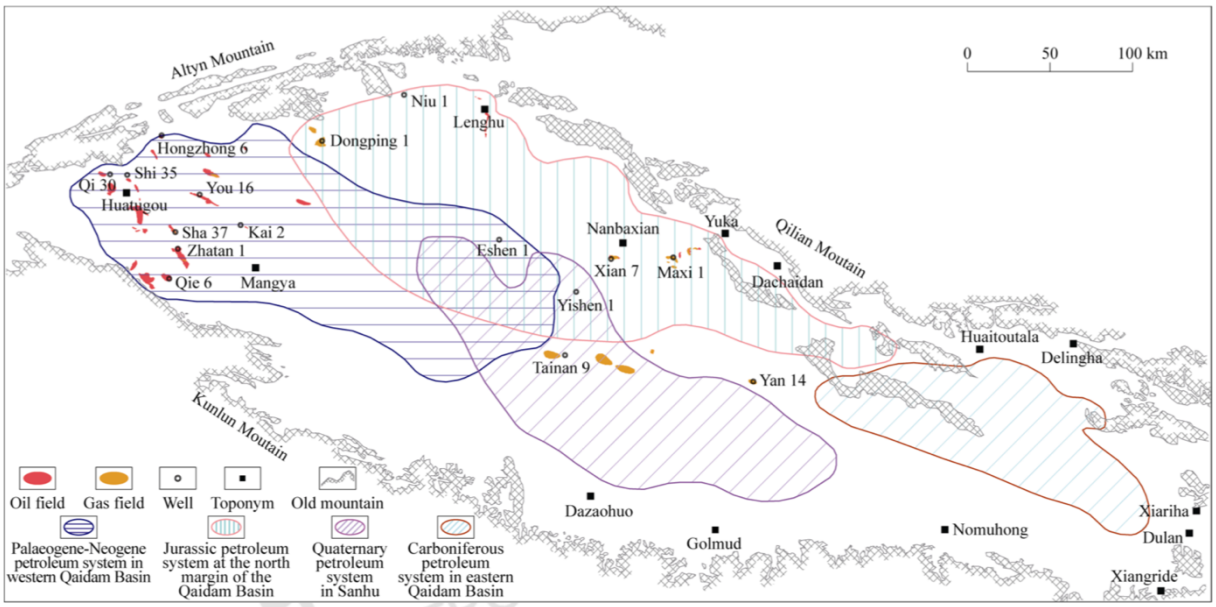

Figure 3.5 Petroleum systems and oil and gas fields within the Qaidam Basin (S. Fu, 2016)

Most papers, including (S. Fu, 2016), (Gu Shusong & Di Hengshu, 1989), (Q. Wang & Coward, 1990), and the United States Geological Survey (Lee, 1984), broadly lump the major oil and gas producing regions of the Qaidam basin into three main groups, the Northern block faulting zone (located in the Northeast of the basin), the Mangya Depression (located in the Northwest), and the new Sanhu depression (located in the South West). The Northern block faulting zone source rocks are primarily Jurassic in origin and are conducive to the production of both oil and gas (Lee, 1984). Source rocks found in the Northwestern, Mangya region are Tertiary in age, with deposition of source material starting around 35 million years ago, and can similarly be conducive to both oil and gas production (Q. Wang & Coward, 1990). Source rocks found in the Sanhu depression area tend to be Quaternary in age and thus are generally less thermally mature. These units source the Sanhu depression's hydrocarbon production which, so far, has been exclusively focused on natural gas. Gu and Di (1990) posited that there was no originally deposited source rock in the Sanhu depression, but as the depocenter shifted to the east, a Quaternary formation subsided which became the source rock within the area. In addition to the three major petroleum systems studied and modeled in this thesis, there are several other energy systems present within the basin. However, these additional energy systems' contribution to the total energy stored in the basin is minimal compared to the three major petroleum systems studied in this thesis (Liu et al., 2017). This thesis will explore the resource potential of each of the three major identified petroleum systems in a unified, whole-basin model.

Methods

4.1 Basin Modeling

Since the first commercial exploitation of petroleum, geologists have developed ways to quantitatively forecast the amount and composition of petroleum resources present in a geological area. Basin modeling is the culmination of these efforts, providing a mechanism to computationally integrate geographic, stratigraphic, lithological, petrophysical, geothermal, and chemical data to arrive at a resource estimate. In the past 50 years, basin modeling has transitioned from a crude approximation of basin processes to a robust, quantitative computational approach for predictive resource assessments (Al-Hajeri & Saeed, 2009), (Hantschel & Kauerauf, 2009), (Angevine et al., 1990). Basin modeling is a form of evolutionary modeling and begins at the earliest time noted in the chrono-stratigraphy. From there, the technique models the accumulation of specified sediments and depositional environments over time (Welte, 2002). As the basin model considers the deposition of sediments it also calculates the accumulation of organic material. The basin model proceeds through time to calculate the organic material's maturation into hydrocarbons, including both oil and gas. In this thesis, we use Schlumberger's Petrel 2019 software to build the basin model and Schlumberger's PetroMOD 2019 software to simulate the evolution of the basin. Both are state-of-the-art applications widely used in the industry.

4.2 Data Used in this Thesis

The original stratigraphic data that provided the basis of the model presented in this thesis was generously provided by PetroChina (中国石油天然气股份有限公司). The data was provided in the form of contour maps describing the depth (Z value), and geometry of a subsurface layer within the stratigraphic section. These contour maps were available only in the all-Mandarin applications, GeoMap and Double Fox, and the data resolution was such that only every fifth contour had an associated Z-value. Each successive line represented an increment of 200m in difference of Z-value, yet the initial maps only had Z values linked to lines representing a Z-value divisible by 1000. Z-Values were manually added to contours that lacked them and then the contour lines were exported in plaintext form from GeoMap. Figure 4.1 shows the T4 contour map in GeoMap.

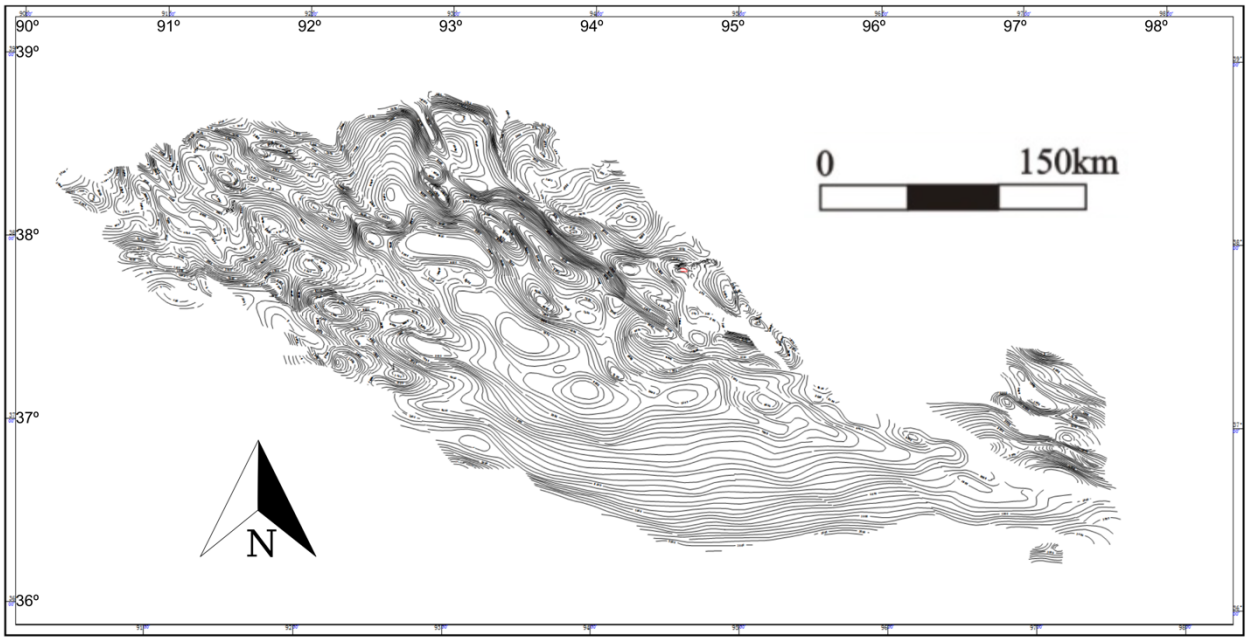

Figure 4.1 T3 Contour Map in GeoMap Software, contour lines represent subsurface geometry in intervals of 200 meters of depth along the z axis

The plaintext files were converted to CSV (comma separated value) files in Microsoft Excel 2018, and they were then processed for formatting in R so that they could be imported into SKUA's GOCAD 2019 software as pointsets. Once imported into GOCAD, these pointsets were converted to surfaces via a least-triangles algorithm. These surfaces were then exported as tsurf files and then imported to Schlumberger's Petrel 2019. Once in Petrel, these mesh surfaces had to be deconstructed again into pointsets and then remade into proper Petrel surfaces that were identified as horizons and correlated to stratigraphic events. Figure 4.2 shows the 3D surface model built in Petrel.

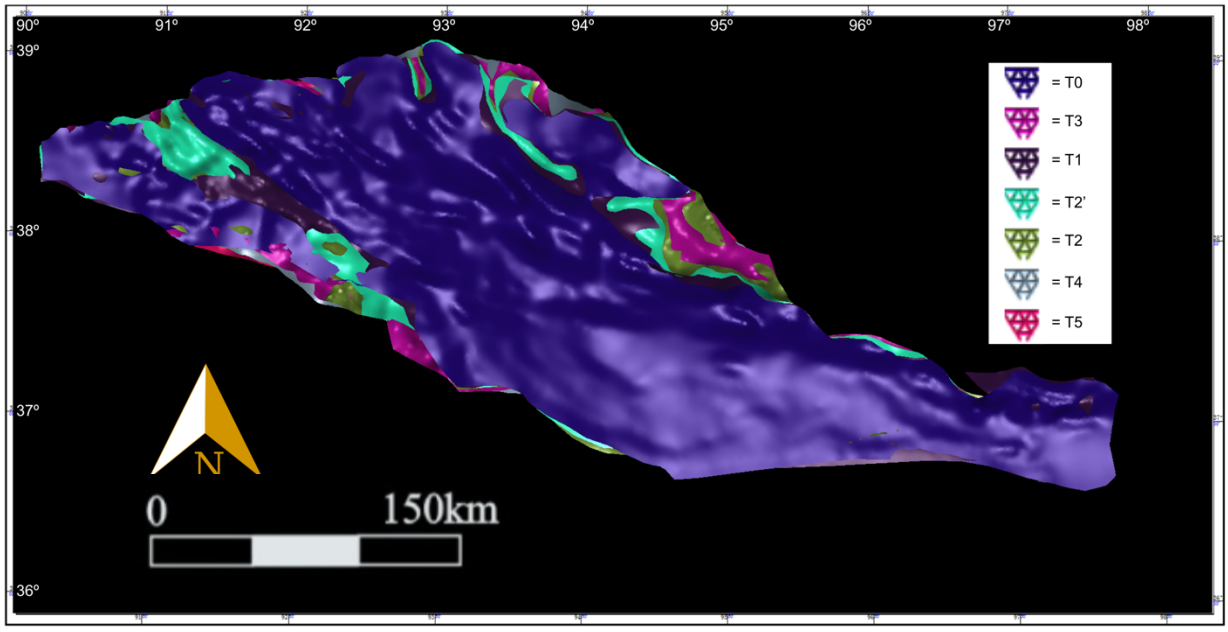

Figure 4.2 Aerial View of 3D Surface Model. Deeper horizons are only partially visible as they are obscured by younger, shallower horizons

Figure 4.2 shows the top down view of all of the 3D horizon surfaces. Deeper horizons are only partially visible as they are largely overlain by younger units. More information on the T# nomenclature can be found in section 3.3.

Other datasets and information essential for the construction of the basin model were assembled from the existing literature on the basin. Examples of these sorts of data points derived from the literature include the basin stratigraphic descriptions (e.g., facies, lithologies), petroleum system boundaries, and geothermal gradients and heat flow values.

4.3 Building the 3D Grid

Essential to any basin model is a grid which represents the subsurface basin geometry. The three-dimensional grid which makes up the skeleton of the model was made in Petrel from the surfaces interpolated from the contour maps provided by PetroChina. The lowest horizon provided by PetroChina was the T5 horizon which represents the top of the Lulehe formation. The T6 and the T7 horizons were created by lowering the T5 horizon by a constant Z-value to represent the bottom of the Lulehe/the top of the Jurassic source rock and the bottom of the Jurassic source rock respectively. The resulting depths of the T6 and 7 horizons were based on the 1984 USGS report which estimated formational layer thickness. Each horizon was then added to Petrel's 3D grid building tool and the grid size was set to 500 m by 500 m. Figure 4.3 shows the 3D gridded model in Petrel.

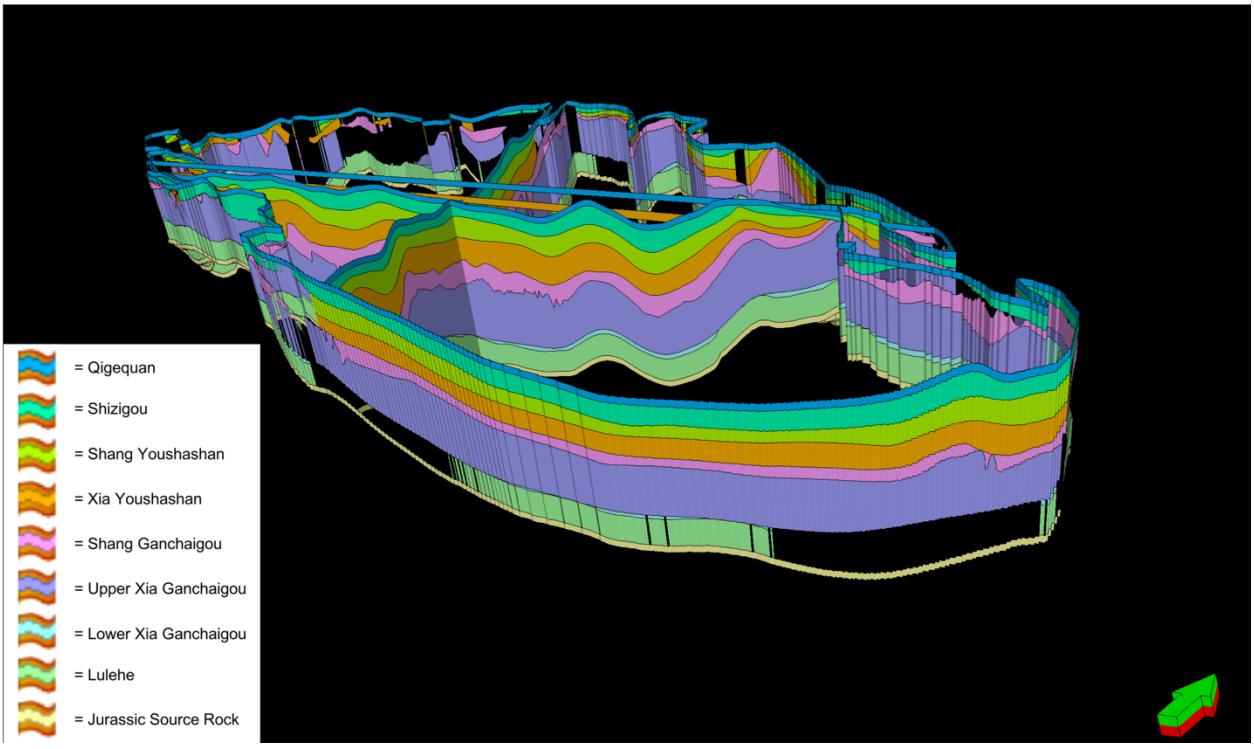

Figure 4.3 3D Gridded Model in Petrel, arrow points North

4.4 Building the Facies Table

A basin model typically includes a table with lithologies and corresponding kinetic and chemical properties for each facies present in the basin. The facies table used for this model was made from compiling data points found throughout the literature on the Qaidam basin's stratigraphy and petroleum system elements. Of particular usefulness were Yanpeng Sun's doctoral dissertation (Sun, 2019) and papers by Fu Suotang (S. Fu, 2016) and Liu Zhanguo (Liu et al., 2017), as well as the 1984 U.S. Geology Survey assessment of the basin (Lee, 1984). Figure 4.4 shows the model with assigned facies and lithologies. The shales and siltstones are source rocks while the sandstones and conglomerates serve as reservoirs for the basin's hydrocarbons. Salt or evaporite layers are common throughout the basin as seals.

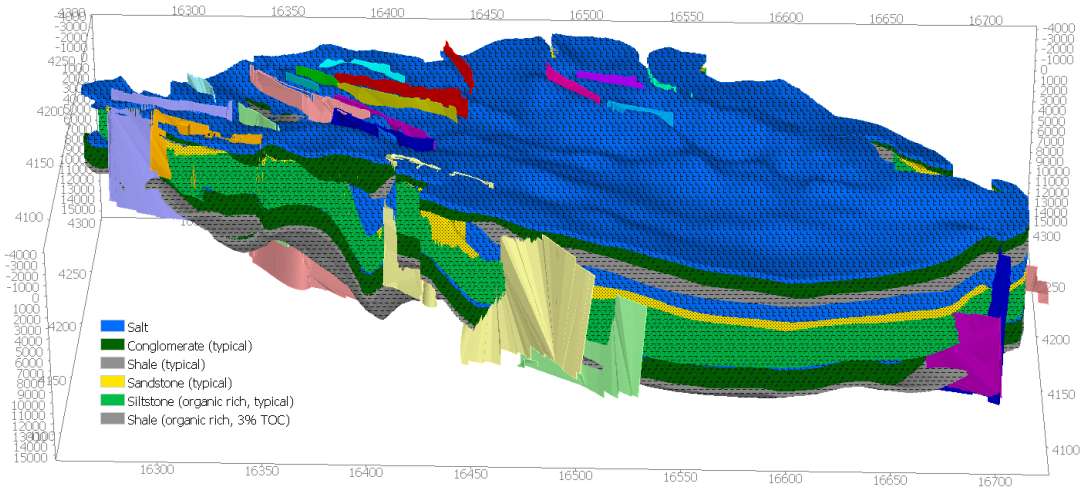

Figure 4.4 PetroMOD Model with Assigned Facies and Lithologies, orange arrow points north, multicolored polygons cutting through the model are fault surfaces

4.5 Modeling in Petrel

The required inputs to build a petroleum systems model via the exploration geology workflow in Petrel are a 3D grid, a facies table, and a fault history. With these objects and properties in Petrel, the software can simulate the deposition of the sediments and generation of hydrocarbons over time. Petrel also requires input of a basal heat flow in milliwatts per square meter. Ordinarily the basal heat flow defaults to 60 mW/m^2 but the literature puts the basal heat flow in the Qaidam basin at 52 mW/m^2 (Hu et al., 2000). To reflect this, a table of heat flow values with associated geological times was created in Petrel via the 'properties' workflow, establishing the proper heat flow in the basin.

An essential step in enabling the model to accurately reflect the petroleum systems was limiting the geographical area of each distinct petroleum system in map view (on the XY plane). The extent of a given petroleum system is generally defined by the distribution of its hydrocarbon source rock. Figure 3.5 in the geologic setting section shows the geographic distribution of the three petroleum systems studied in this thesis as well as a fourth, carboniferous petroleum system not studied here due to a lack of data to define other elements of the petroleum system in the South East part of the basin. In order to adequately model the geographical distribution of source rocks in the basin, a geometrical property was added to the 3D grid. The TOC (total organic carbon) was first set to zero across all rock intervals, and then properties specifying non-zero TOC values derived from existing literature were added to each source rock interval (between the top and bottom of the source rock). These non-zero TOC values were confined to an XY axis polygon that reflected the extent of the corresponding source rock. This was done for the Jurassic source rock, the Paleogene-Neogene source rock, and the Quaternary source rock.

4.6 PetroMOD Simulations

Once the model was built in Petrel, it was exported to PetroMOD where the basin simulation could be run. Initial models ran into issues with the seal rocks not adequately confining the hydrocarbons. In order to fix this, custom lithologies were built in PetroMOD's lithology editor and then updated in PetroBuilder 3D. These custom lithologies were built to represent the evaporite layers present throughout the Qaidam basin which act as seals to the basin's petroleum systems. Once the lithologies were sorted out, the model could be built and saved in PetroBuilder 3D and the simulation could be run. The model was run more than eighty times in total, with each model testing different parameters and trouble-shooting technical issues. Once technical issues were resolved, essential model inputs and their ranges were aggregated from the existing literature. This thesis presents a primary model, termed the 'flagship model,' which most accurately reflects our understanding of conditions in the basin. Once the flagship model conditions and properties were established from the literature, the model was run many more times to test its sensitivity to many key properties including basal heat flow, fault activity periods, fault permeability properties, total organic carbon (TOC), and hydrogen index. Figure 4.5 shows the flagship model in PetroMOD.

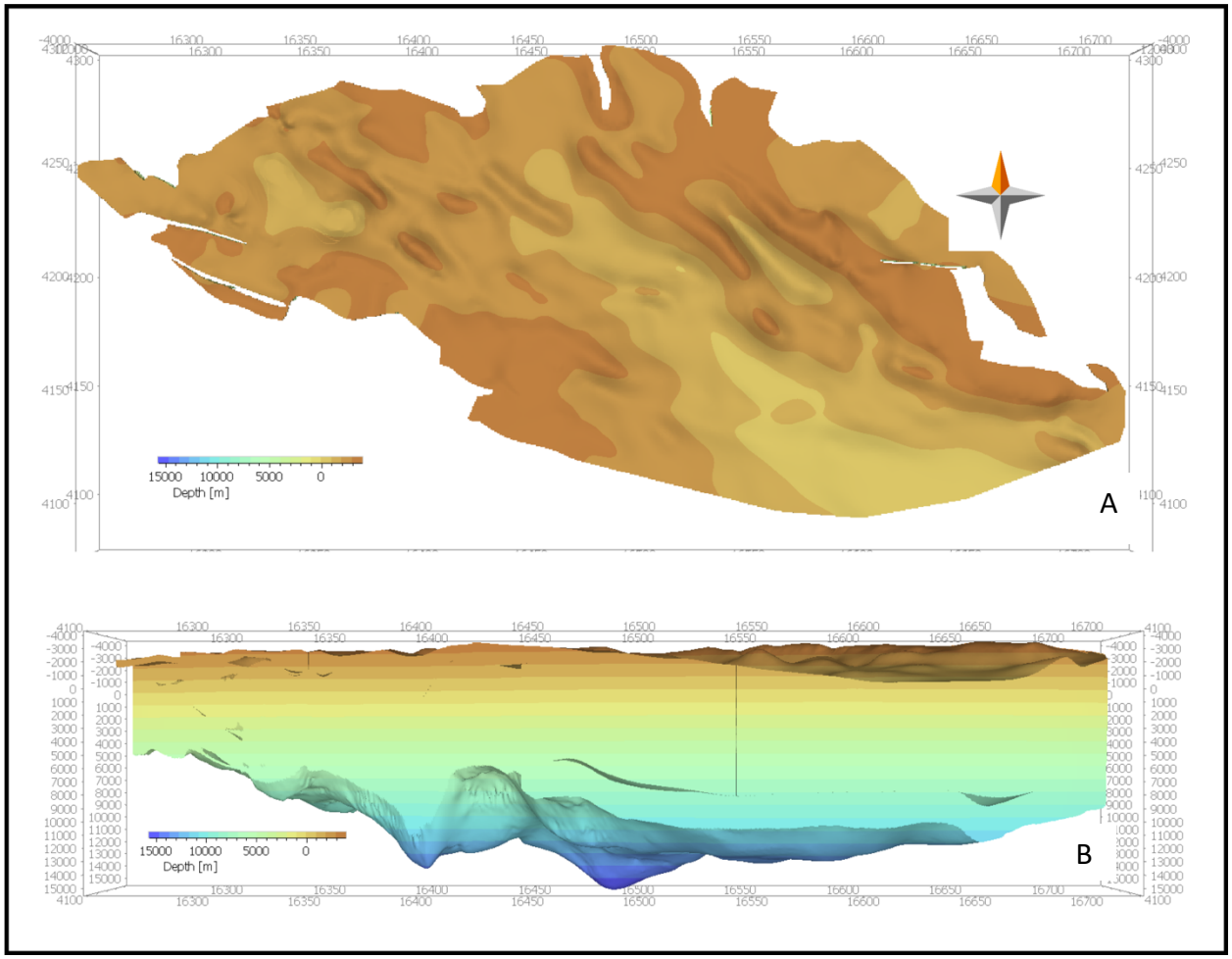

Figure 4.5 Flagship Model in PetroMOD with Depth Property. A – View from the top down. B – View of the basin from the south

4.7 Validation of Combined Petroleum Systems Modeling Method

The basin model was run over 80 times in PetroMOD to fully debug, calibrate, and test model and simulator parameters. Each model run took about 1.5 hours on a Dell Precision Tower 5810 with an Intel Xeon E5-1607 v3 3.1ghz processor and 32 gigabytes of RAM running 64-bit windows 7. By the 81st run, the model was fully calibrated, and the parameters were suitably adjusted so as to most accurately reflect geological conditions in the basin throughout its history. This version of the model and subsequent simulation results will be referred to as the flagship model run.

When building the model and defining petroleum system elements, an essential question remained as to the validity of defining petroleum system elements throughout the basin. Each depositional layer could only be classified as a single petroleum system element, either a source rock, reservoir, seal, overburden rock, or under-burden rock. However, throughout the basin, many formations, such as the Quaternary shales, act as both source rocks and as seals for separate petroleum systems. As such it is necessary to examine the validity and impacts of simplifying each rock layer, defined as the grid between stratigraphic horizons, into a single petroleum system element. The flagship basin model was run three times, in each case with a different facies table and a different assignment of petroleum system elements corresponding to each of the three separate major petroleum systems in the basin. These three simulation-runs produced aggregate results very similar to the results found in the flagship model's approximation of hydrocarbon reserves. While the flagship simulation produced 7.69 gigatons on hydrocarbon resources, the three individual petroleum systems models combined produced 8.68 gigatons, an increase of only 13% over the flagship model, with a spatial distribution of hydrocarbon accumulations very similar to that found in

the flagship model. It was expected that the aggregate resource accumulations of the three individual petroleum systems models would be greater than those of the flagship model given that the limiting factor on hydrocarbon accumulations in the basin is not hydrocarbon generation but rather trap size and reservoir space. In the three individual petroleum systems models, there was more reservoir availability for hydrocarbon storage for the small percent of hydrocarbons which escaped the primary reservoir/seal pairing and migrated to an above reservoir rock. However, in the actual basin, as in the flagship model, it is likely that these same hydrocarbons are competing for reservoir space, which explains the discrepancy between the sum of the individual petroleum system runs and the flagship model.

Results

5.1 Numerical Simulation Results

The flagship model, when run through simulation in PetroMOD, yielded a total mass of 7.69 gigatons of oil and natural gas accumulated throughout the basin's reservoirs as geological resources. Our results represent a 25% increase over the resource assessment of the entire Qaidam Basin published by Fu (2016), which found 6.17 gigatons of hydrocarbon geological resources and a 205% increase over the resource assessment published by Jiang et al. in 2015, which found 2.47 gigatons of total geological resources. Figure 5.1 provides context for these various resource assessments by examining oil and gas resource assessments of China's largest inland basins.

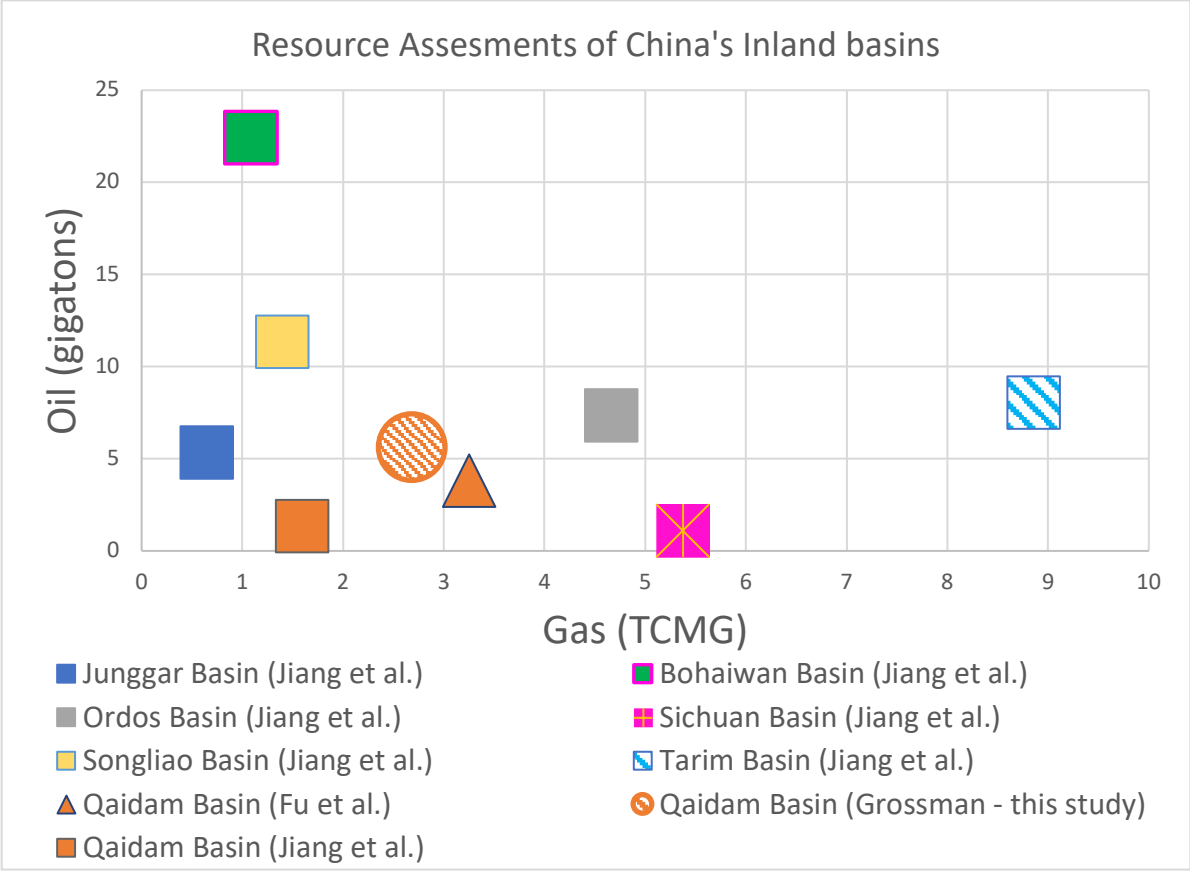

Figure 5.1 Resource Assessments of China's Major Inland Petroliferous Basins

The flagship model results suggest a total natural gas resource of 95 TCFG or 2683 BCMG. This is 17% lower than Fu et al.'s resource estimate of 3248 BCMG and a 16% lower than Zheng et al.'s resource estimate of 3213 BCMG (Zheng et al., 2018); however, it is a 68% increase over the resource assessment of 1600 BCMG published by Jiang et al (Jiang et al., 2015). This model provides strong support for the more recent natural gas resource assessments of Fu and Zheng over the earlier, more conservative estimate in Jiang et al. Figure 5.2 shows the chronological accumulation of oil and gas throughout the basin's reservoirs. It is also notable that this model likely represents a conservative estimate, given that simulating each petroleum system individually yielded a greater resource mass by approximately 13%.

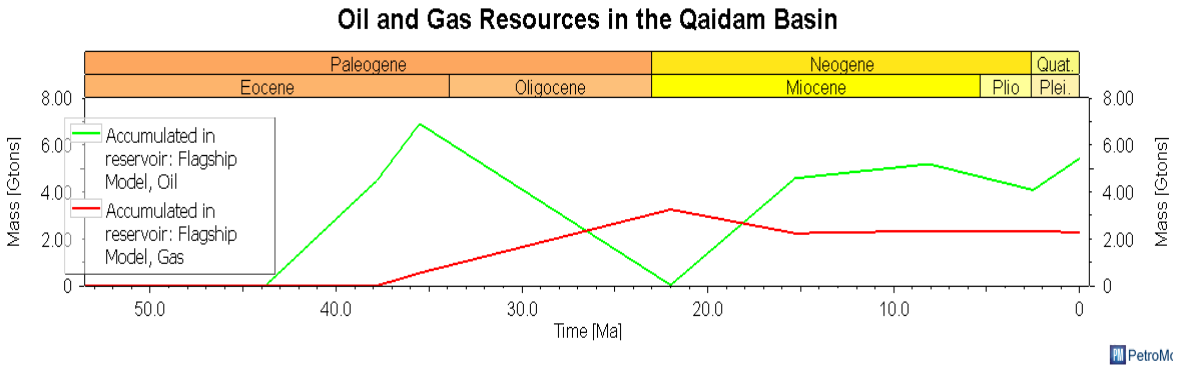

Figure 5.2 Total oil and gas resources in the Qaidam basin over time

The amount of variance in simulation results suggests dependencies on several key model parameters that must be considered to assess the uncertainty in these outcomes. As can be seen in figure 5.2, altering fault properties or basal heat flow can increase the geological resource estimate substantially. Of particular interest are the higher than expected numbers in terms of oil resources. Fu et al. estimates an original oil resource of 27.85 billion barrels

between the three petroleum systems considered in this thesis, whereas the flagship model suggests a total oil resource of 39.43 billion barrels, an increase of 41.5% over Fu's numbers (S. Fu, 2016). Furthermore, the flagship model produces one of the lowest estimates of total oil resources compared to other model runs, which suggests the flagship model's result may be a conservative estimate of the basin's total oil resources. Figure 5.3 shows the different resource estimates produced by varying several key model parameters.

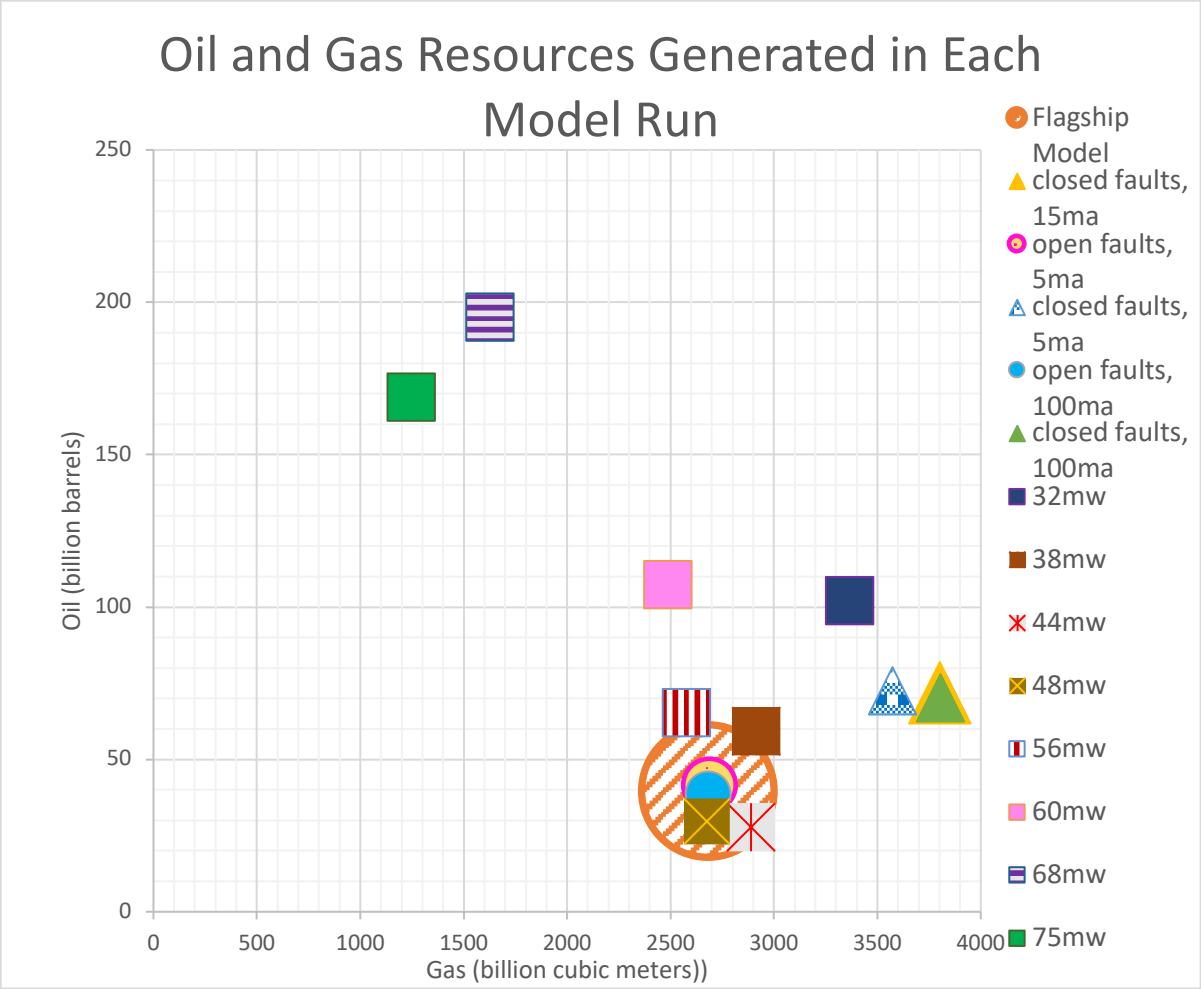

Figure 5.3 Oil and natural gas resources generated across different model parameters. In the legend, mw stands for milliwatts and ma stands for million years ago. Orange circle represents flagship model conditions throughout. Key flagship conditions include fault activity beginning 15 million years ago, open faults, and a heat flow of 52 mW/m^2

In the following sections, we discuss several key model parameters including basal heat flow, fault properties, hydrogen index and TOC, and their effect on modeled resource accumulation.

5.2 Model Sensitivity to Basal Heat Flow

One of the most essential inputs for any petroleum systems model is heat. Heat is often measured, particularly for 1D and 2D models, in terms of geothermal gradients. When making a 3D petroleum systems model in Petrel however, one needs to input heat flow in the form of basal heat flow over time. The basal heat flow represents the amount of heat energy per square meter of surface that is constantly radiating from the Earth's interior underneath the given surface area. The average basal heat flow across the world, and thus a common default heat flow, is 60 mW/m^2. Hu et al. in their 2000 paper, "Heat flow in the Continental Area of China: A New Data Set," suggest a basal heat flow of 52 mW/m^2 throughout the Qaidam basin. However, the range of potential heat flows described in their paper varies from 32 – 75 mW/m^2. As such it is difficult to choose an appropriate heat flow for the entire region, particularly given that heat flow is likely heterogeneous throughout the basin. This flagship model takes Hu et al.'s closest approximation of 52 mW/m^2 and applies that heat flow to the whole basin. In order to precisely model generation, however, heat flows would need to be tested through the basin both spatially and temporally. Given the lack of information to constrain such variations, we chose to test a range of constant heat flow values to explore the sensitivity of our results to this parameter. Figure 5.4 shows the relationship between total geological resources and basal heat flow

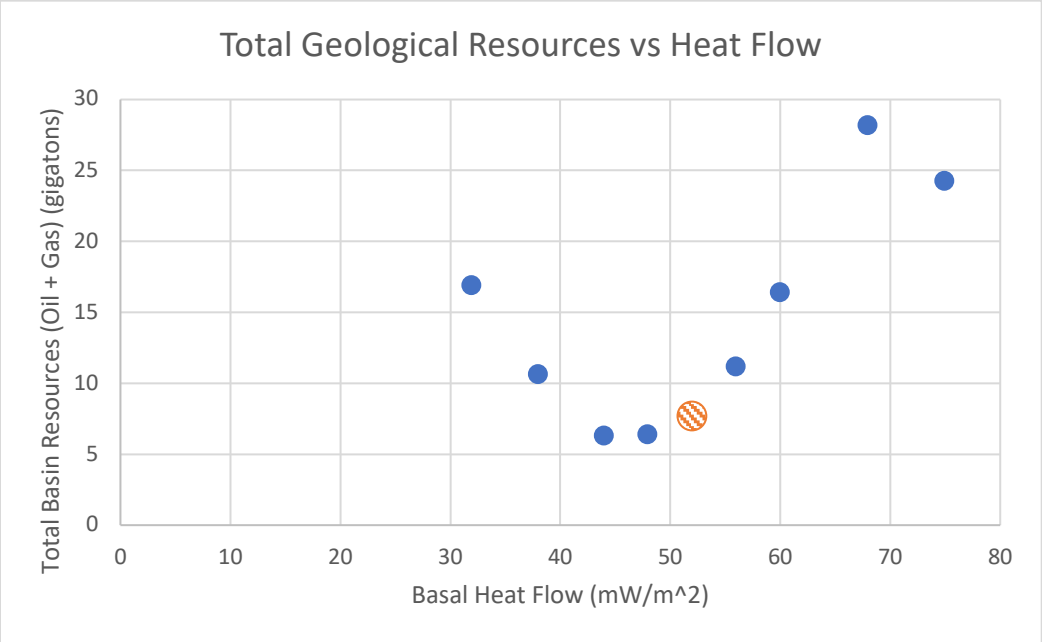

Figure 5.4 Total Mass of Geological Resources vs. Basal Heat Flow, orange circle indicates flagship model condition of 52 mW/m^2

It is of particular note that the relationship is not linear, in fact the trend of the relationship varies as a function of the heat flow. Increases of basal heat flow from about 30 to 45 mW/m^2 yield a decrease in hydrocarbon resources, whereas increases above 45 mW/m^2 yield an increase in resources. This may seem counter intuitive. However, I suggest that this happens since the Jurassic petroleum system in the northeast of the basin has many of its hydrocarbons overcooked and rendered useless given the Jurassic source rock's great depth and relatively old age. However, when the heat flow is lowered to 32 mW/m^2 a great portion of the Jurassic hydrocarbons that were overcooked under previous scenarios are converted into oil and gas and accumulate in reservoirs without leaking or being overcooked. In every model iteration the productivity of the Jurassic petroleum systems is inversely correlated with heat flow, whereas the Paleogene and Quaternary petroleum systems' productivity is positively correlated with basal heat flow. This only goes up to a point, however, as can be

seen from the resource maximum at 68 mW/m^2. I hypothesize that once the heat flow is greater than 68 mW/m^2 the Paleogene source rock gets partially overcooked and as such, 68 mW/m^2 is the heat flow which maximizes basin-wide hydrocarbon accumulation.

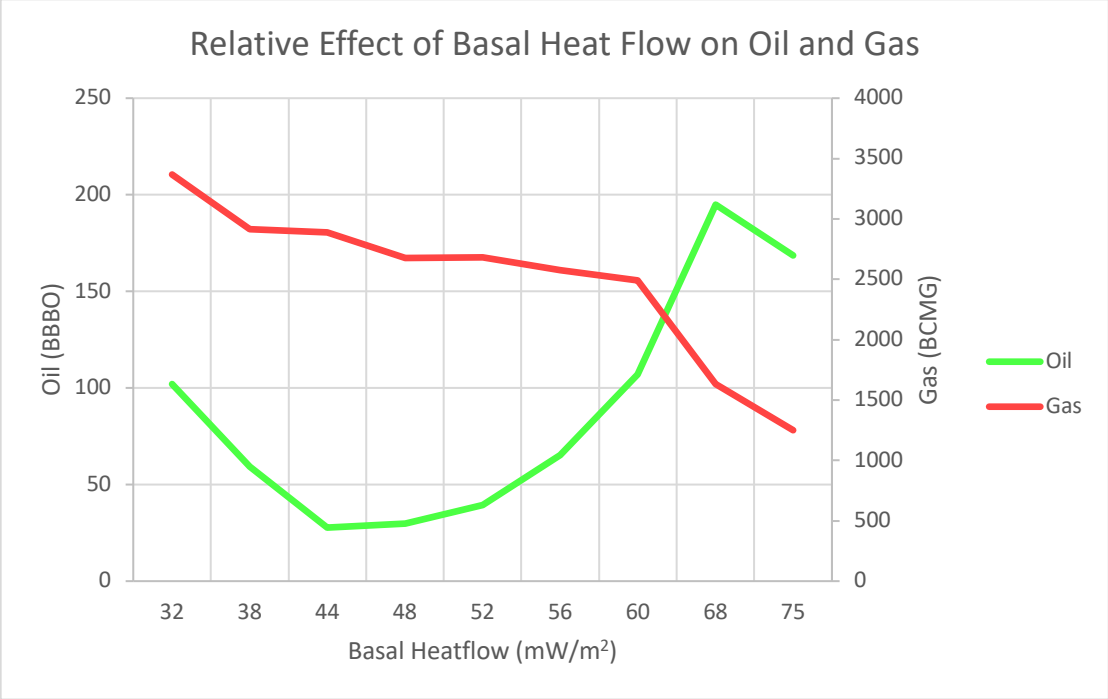

Figure 5.5 Relative effect of basal heat flow on oil and gas accumulation

Figure 5.5 delves into the relationship between the relative production of oil and gas and heat flow. Here we can see how the 32 mW/m^2 heat flow model produces substantially more gas than any other model, which makes sense given that the Jurassic petroleum system primarily generates natural gas. The natural gas trend is well explained by the Jurassic petroleum system behavior just described, as it can be seen that the maximum heat flow results in the minimum gas resource generation. Conversely, gas generation and accumulation are maximized by decreasing the heat flow.

5.3 Model Sensitivity to Fault Properties

Fault properties were another potentially significant variable in the simulation series. The two properties tested were the age of the fault activity and the fault permeability. The majority of faulting activity throughout the basin occurred during the Cenozoic (Wu et al., 2014). This is demonstrated by the presence of syntectonic growth strata imaged in seismic reflection data and identified in wells. Growth strata typically thin onto structural highs generated by faulting, whereas pre-growth (or pre-tectonic) strata do not record such uplift (Sun, 2019). The first major, regional growth horizon in Qaidam is the Shang Youshashan formation which began deposition approximately 15 million years ago (mya). Additionally, Wu et al. (2014) suggest that the Cenozoic faults throughout the Qaidam basin tend to have high permeabilities and are generally conducive to the flow of hydrocarbons (Wu et al., 2014). As such, in the flagship model the faults are open and begin activity at 15mya. While fault timing and properties are well documented in these referenced studies, it remains important to understand the robustness of model results relative to potential variance in fault properties. Figure 5.6 details the relationship between fault age and hydrocarbon accumulation in the Qaidam basin, separating between simulation runs with open and closed faults.

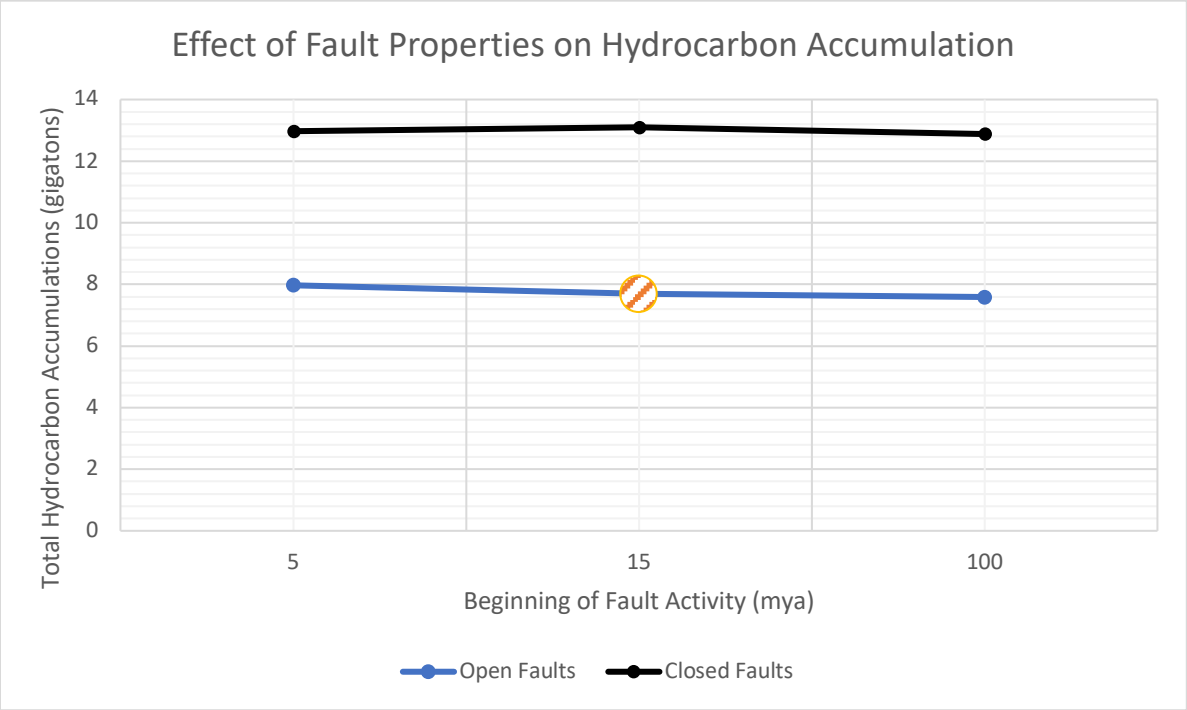

Figure 5.6 Effect of fault properties on hydrocarbon accumulation, orange circle represents flagship model conditions of fault activity beginning 15 million years ago and faults being open

As can be seen from figure 5.6, the fault property with a greater impact on resource accumulation is fault permeability rather than the age at which faulting began. Future model runs could be improved in accuracy by taking into account local knowledge about fault behavior and defining numerical fault permeabilities on a case by case basis rather than labelling all of the faults open. Nevertheless, the inputs to our flagship model reflect the general, current understanding of fault properties in the basin, and thus should be considered to yield viable results.

5.4 Model Sensitivity to Total Organic Carbon and Hydrogen Index

Total organic carbon (TOC) within source rocks and hydrogen index (HI) were by far the two most influential factors on total hydrocarbon resource accumulation. A 50% decrease in either TOC or HI resulted in a corresponding 50% decrease in total hydrocarbon accumulations. As such, the essential consideration becomes defining a reasonable range of these properties. Appendix A contains a table of assumed TOC and HI values and their sources. For each source rock interval, a low, median, and high value were gathered from the literature. The flagship model used median values of TOC and HI but models with HI and TOC varied to low and high estimates are depicted below in figure 5.7, designed to provide an understanding of the range of possible resource estimates for the Qaidam basin.

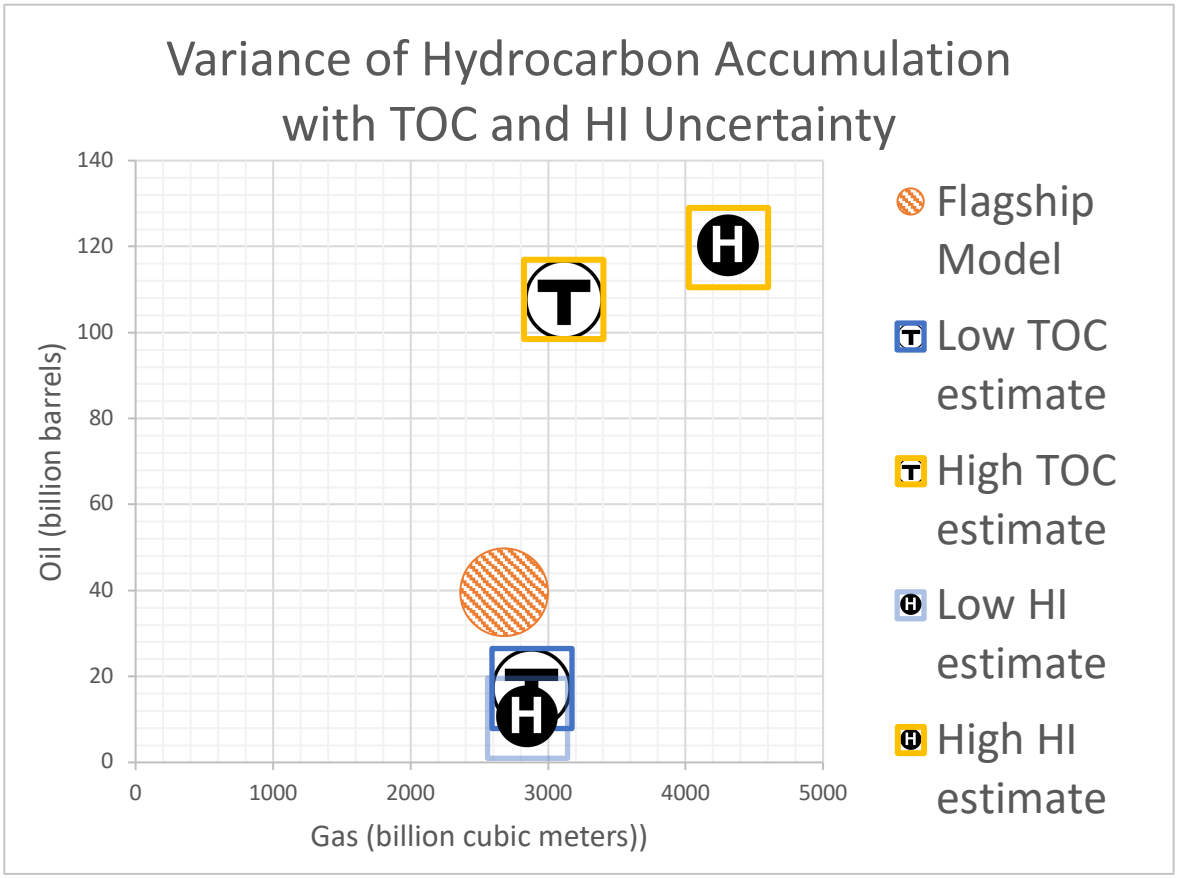

Figure 5.7 Variance of hydrocarbon accumulation with TOC and HI uncertainty

It is of note that the high and low TOC and HI estimates are not symmetrically located around the flagship model. While the low estimates decrease the oil resources by about 50-75%, the high estimates increase the oil resource estimate by 150-200%. Similarly, while low TOC/HI estimates do not meaningfully decrease the volume of gas accumulated, high estimates increase this result significantly. This implies that the flagship model is conservative in its resource assessment. Ultimately, TOC and HI are incredibly influential factors in the resource assessment and further refining estimates of these properties could have profound impacts on our understanding of the total resources present in the basin.

5.5 Spatial Results

The PetroMOD results not only produce an estimate of the mass of hydrocarbons accumulated in reservoirs throughout the basin; model results also provide a prediction of the hydrocarbon distribution through the basin. (Figure 5.8)

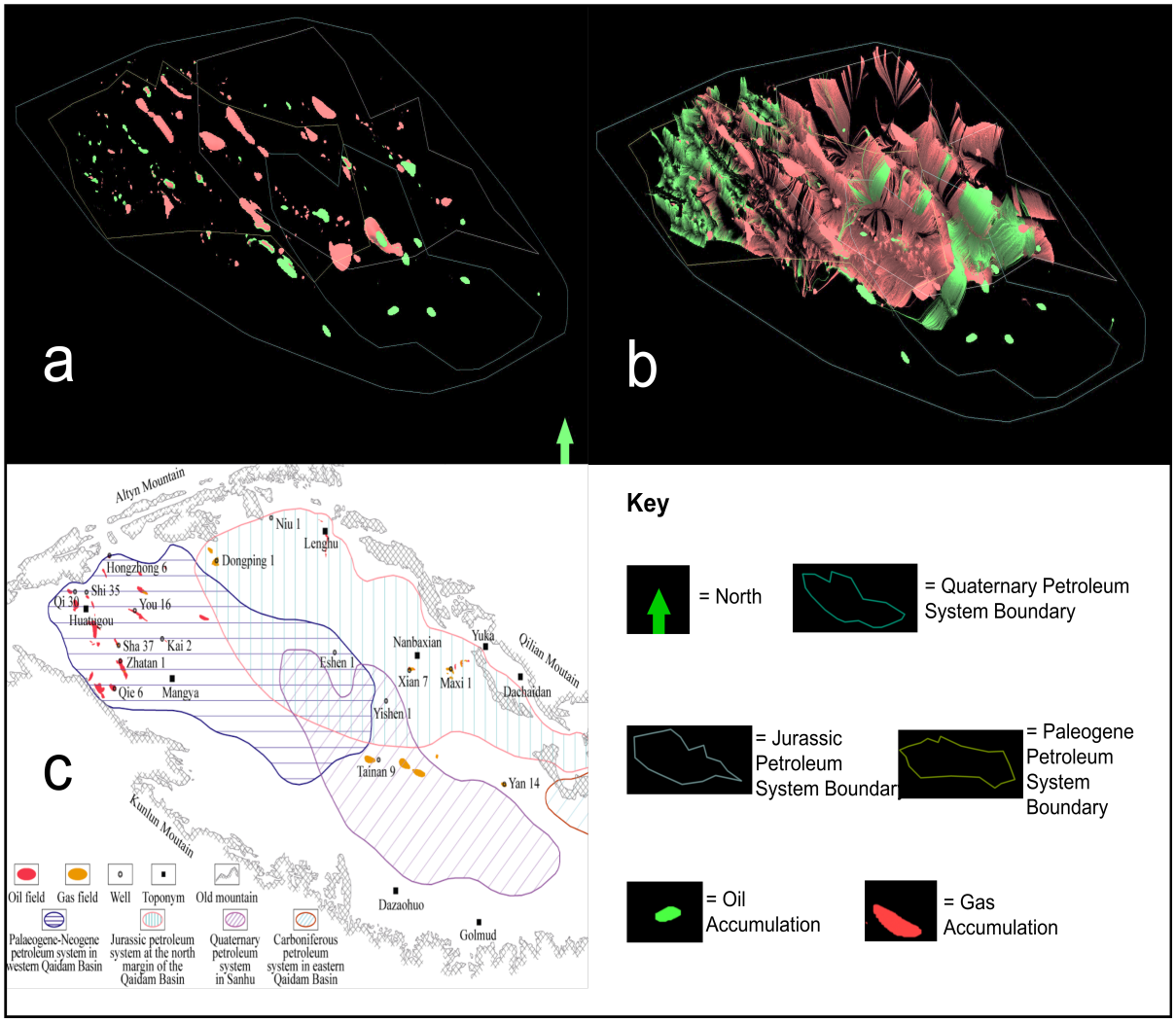

Figure 5.8 Map of hydrocarbon accumulations simulated by flagship model. Red represents natural gas while green represents oil. A – Modeled oil and gas accumulations throughout the basin. B – Modeled oil and gas accumulations with associated flow paths. C – Reference figure with oil and gas fields from (S. Fu, 2016)

Spatial results visualized in figure 5.8a and 5.8b can be compared against the reference figure, 5.8c from Fu et al. to gauge the geographically predictive accuracy of the model's results. The high concentration of oil fields to the northwest of the basin is reflected in the series of green regions of oil accumulations shown in figure 5,8a and 5.8b. Similarly, the large, red accumulations of simulated natural gas in figure 5.8a and 5.8b are reflected in the gas fields in the center of the basin shown in 5.8c. While this is one of the coarser estimates presented, given that the model does not accurately simulate individual traps, it is nonetheless valuable as a tool with which to confirm the validity of the model. As can be seen from figures 5.8a, b, and c, the model produces accumulations which can be confirmed by the presence of actual petroleum fields throughout the basin. This helps to confirm the robustness of the model and its parameterization.

Discussion

6.1 Qaidam's Future Development

Qaidam has a bright future as one of China's major petroleum producing basins. Resources are abundant and the infrastructure is in place to extract them. The major questions of the basin's future development are centered around total basin resources, future infrastructure development, and the future of China's energy economy. This resource assessment provides strong support for the more recent natural gas resource assessments of (S. Fu, 2016) and (Zheng et al., 2018) over the earlier, more conservative estimate of (Jiang et al., 2015). This resource assessment also suggests that previous resource assessments of the basin have underestimated the total present oil resources.

While current field size distribution data and the precise geographical distribution of active oil and gas fields is not publicly available due to national energy security concerns, several figures from the literature indicate some of the known oil and gas field locations. Many of these locations are only known to first order, i.e. it is known that there is substantial oil exploitation in the Northwest of the basin, yet the exact locations of wells and field sizes remain confidential. Excluding the known areas of development, such as the oil fields in the basin's Northwest and the Gas fields in the South of the basin, our results point to several areas which are likely yet to be fully exploited, and perhaps the resource potential of which has been historically underestimated. Figure 6.1 shows the geographical distribution of oil and gas resources in the basin as simulated by the flagship model, separated by reservoir interval.

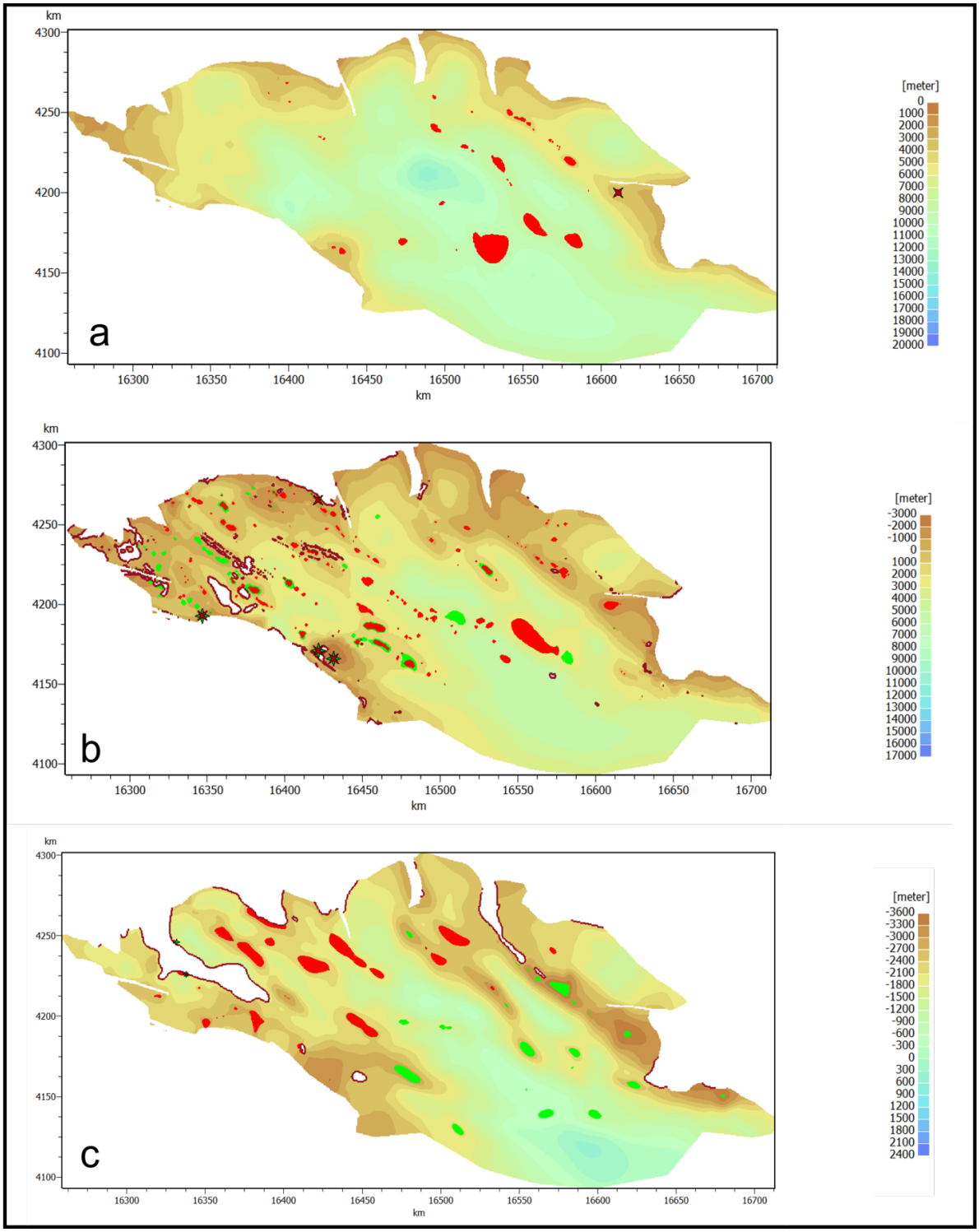

Figure 6.1 Hydrocarbon accumulation maps separated by petroleum system. Red represents natural gas while green represents oil. Bars to the right indicate elevation. A – Oil and gas accumulations in the Jurassic petroleum system. B – Oil and gas accumulations in the Paleogene petroleum system. C – Oil and gas accumulations in the Quaternary petroleum system.

In general, there is greater than expected gas resource accumulation in the West of the basin, and greater than expected oil resource accumulation in the South of the basin. It also appears that there may be more gas accumulation than expected in the Northwest of the basin, or the Mangya area. This is gas originating from Jurassic source rocks and as such may require deeper drilling than the Paleogene and Quaternary oil plays that have been and are presently being exploited in that area. It is difficult to reach further conclusions due to lack of field distribution data, however it is anticipated that the spatial results provided in this thesis will provide insight to those with this data who are seeking to efficiently take advantage of the Qaidam basin's many conventional resources.

A major question remains as to the future development of tight oil and tight gas stored in the shales around the basin (G. C. Wang et al., 2018), but development of these resources likely won't begin until economic conditions make the technically challenging and resource intensive drilling for tight oil and gas viable. Marginal extraction costs in the Qaidam basin are high, due to the basin's remote location and high elevation, which has kept large scale hydraulic fracturing, or fracking, from being economically viable thus far.

6.2 Implications of Numerical Gas Results

Natural gas resource estimates and further down the line, reserve estimates, are of critical importance in China, given the pressure the domestic gas supply faces. As natural gas takes up a greater and greater share of China's total energy mix these fundamentally geological questions will only grow in importance. Flagship model results imply a total natural gas resource of 2.68 trillion cubic meters (TCMG) or 94 trillion cubic feet (TCFG), supporting the recent natural gas resource assessments of (S. Fu, 2016) and (Zheng et al., 2018) over the earlier, more conservative estimate of (Jiang et al., 2015). This is a generally positive outlook to those seeking to increase China's natural gas reserves.

All of the economically recoverable natural gas in the Qaidam basin is expected to be competitive with imports going forward. Qaidam already provides 5% of China's annual gas supply and the yearly gas exports from the basin will likely only increase over the next decade. As China continues to replace coal with gas and China's gas demand thereby increases, Qaidam's contribution as a share of yearly gas usage may shrink, yet the basin will remain a key area for development in the context of domestic gas production, which will be essential if China seeks to curb dependency on imported gas.

6.3 Implications of Modeled Oil Results

The flagship model results indicate a significantly greater total oil resource than has ever been estimated of the Qaidam basin. Such a result is significant for both local oil prices as well as for China's general energy security. As China is a net importer of oil, it is expected that the oil produced from the Qaidam Basin will be sold domestically. However, it is important to take China's changing energy economy into account. Oil produced in Qaidam will be competing with imported oil, particularly from the middle east and Africa. Figure 6.2 depicts the geographic distribution of China's oil imports.

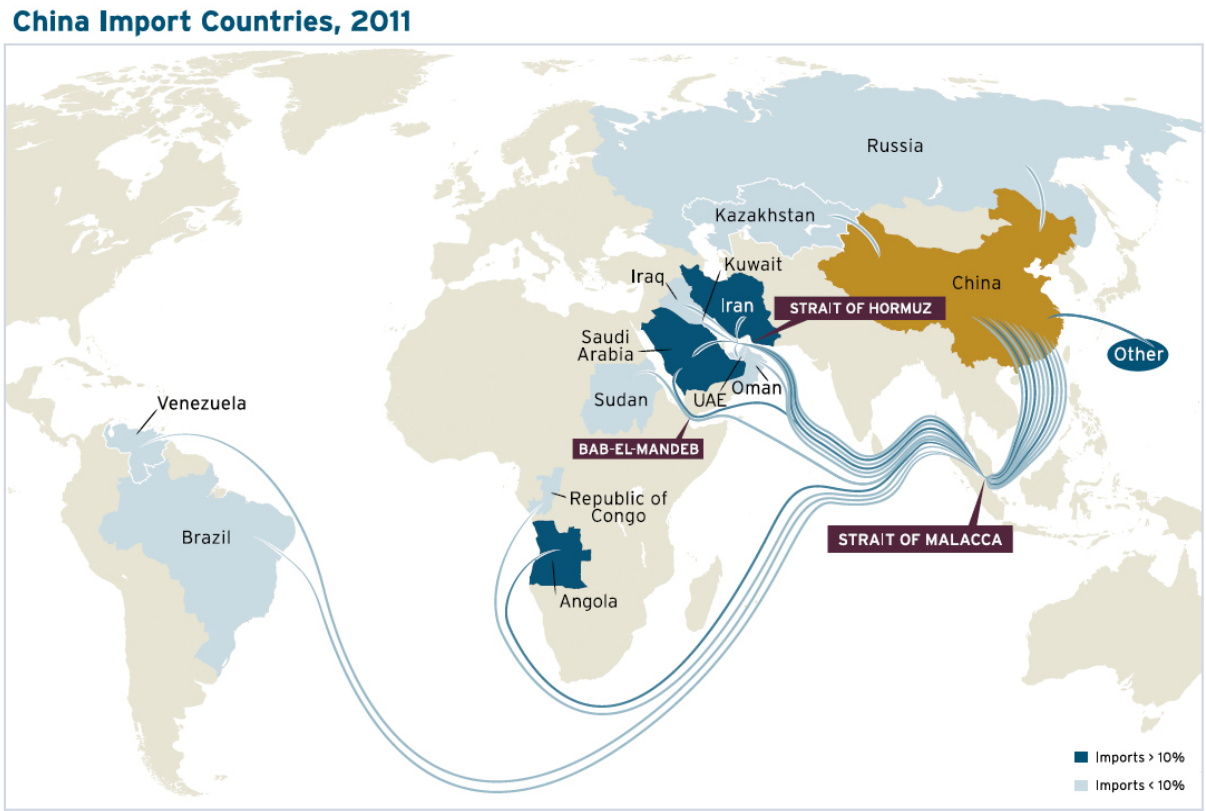

Country	Saudi Arabia	Angola	Iran	Russia	Oman	Iraq	Sudan	Venezuela	Kazakhstan	Kuwait	UAE	Brazil	Republic of Congo	Other
Percentage of Imports	19.8	12.3	10.9	7.8	7.2	5.4	5.1	4.5	4.4	3.8	2.7	2.6	2.2	11.3
Thousand Barrels	366,825	227,395	202,575	144,175	132,495	100,740	94,900	83,950	81,760	69,715	49,275	48,910	41,245	208,780

Figure 6.2 Map of China's Oil Imports (Underwood, 2012)

It is fairly obvious when comparing figure 6.2 and figure 1.3 from section 1.4 that there is a great amount of similarity between the geographic distribution of the Belt and Road Initiation (BRI) and the geographic distribution of China's sources of oil imports. As the BRI grows and changes the way in which China trades, it is likely that oil and natural gas imports will be streamlined, and transportation costs will fall significantly as more transportation infrastructure is built between areas of oil production and China's Eastern and Southern ports. As this change gradually occurs, I theorize that the oil being extracted from the Qaidam basin may become less economically competitive with foreign sources of oil, particularly in Eastern China, which is far from Qaidam. Qaidam's oil, due to the high transportation costs associated with the Tibetan plateau, will likely be used locally in the West of China or possibly even exported via Kazakhstan, Kyrgyzstan, or Mongolia. Given the domestic petroleum production capabilities and limited market demand China's neighbors to the west, it is very possible that oil exported from Qaidam could eventually reach Europe. It is also distinctly possible that the oil extracted from Qaidam may be used in plastics and petrochemical manufacturing locally. Increasing manufacturing in the area could stimulate the local economy and decrease transportation costs. Pipeline is being built every day in Qaidam and its surrounding area and the future is full of possibility.

Conclusions

While there have been a handful of papers which offer resource estimates of the oil and gas present in the Qaidam Basin, this thesis presents the first assessment that is supported by a fully documented and transparent, state-of-the-art whole basin model. Thus, this study offers the first methodologically transparent resource assessment of the Qaidam Basin. The resource estimate presented in this study indicates key areas for future exploration and suggests a much greater total oil resource than has been predicted previously. There are several key areas for future development indicated by the spatial distribution of oil and gas accumulations and knowledge of existing oil and gas fields. The two largest key areas include the northwestern Mangya depression as a hub of future gas generation, and the Southern Qaidam basin, near the Sanhu depression, as a source of future oil production. High quality resource estimates are becoming increasingly important as Chinese energy demand grows, and China looks to increase domestic production. This study indicates that the Qaidam Basin is a particularly attractive target for increasing domestic oil and natural gas production – model estimates indicate that the basin is largely underdeveloped with respect to natural gas. Qaidam's natural gas resources will undoubtedly be used to help support China's ongoing efforts to reduce its use of coal as a way to address urban air pollution. While the oil produced in the Qaidam basin may be difficult to transport to the main hubs of China's oil demand to the East and South, the oil produced in Qaidam could be exported, used domestically in the West, or used in plastics manufacturing or other heavy industries.

- This study confirms the validity of the more recent, higher natural gas resource assessments of Fu and Zheng over the earlier, more conservative estimate in Jiang et al.

- This study suggests a total oil resource of 39.43 barrels in the Qaidam Basin, which is 40% than has previously been estimated.
- Key areas for future development of gas include the northwest Mangya depression and the southeast of the basin.
- Key areas for future development of oil include the southern area of the basin, near the Sanhu depression.

References

Al-Hajeri, M., & Saeed, M. Al. (2009). Basin and Petroleum System Modeling. *Oilfield Review*, (June).

Angevine, C. L., Heller, P. L., & Christopher, P. (1990). Quantitative sedimentary basin modelling. *AAPG Continuing Education Course Notes*, *32*, 103pp.

Besson, C., Pflüger, A., Ahlbrandt, T., & Amano, T. (2003). Resources to Reserves.

China National Petroleum Corporation. (n.d.). *Qaidam Basin*.

Clemente, J. (2016). China's Rising Natural Gas Demand, Pipelines, and LNG. *Forbes*, 1–11. Retrieved from http://www.forbes.com/sites/judeclemente/2016/04/24/chinas-rising-natural-gas-demand-pipelines-and-lng/#7cf6dfc46a38

Eder, T. (2018). Mapping the Belt and Road initiative: this is where we stand. Retrieved from https://www.merics.org/en/bri-tracker/mapping-the-belt-and-road-initiative

Fu, B., & Awata, Y. (2007). Displacement and timing of left-lateral faulting in the Kunlun Fault Zone, northern Tibet, inferred from geologic and geomorphic features. *Journal of Asian Earth Sciences*, *29*(2–3), 253–265. https://doi.org/10.1016/j.jseaes.2006.03.004

Fu, S. 付锁堂 (2016). 柴达木盆地油气勘探新进展，Potential oil and gas exploration areas in Qaidam Basin. *China Petroleum Exploration*, *21*(5), 1–11.

Gu Shusong （顾舒松）, & Di Hengshu （狄恒恕）. (1989). 柴达木盆地形成机理及其对油气的控制， Mechanism of formation of the Qaidam Basin and its control on petroleum. *Chinese Sedimentary Basins*, 45–51.

Guo, A., Murtaugh, D., & Stapczynski, S. (2018). China increases natural gas imports to avoid winter shortage.

Hantschel, T., & Kauerauf, A. I. (2009). *Fundamentals of basin and petroleum systems*

modeling. *Fundamentals of Basin and Petroleum Systems Modeling*. https://doi.org/10.1007/978-3-540-72318-9

Hu, S., He, L., & Wang, J. (2000). Heat flow in the continental area of China : A new data set, (October 2017). https://doi.org/10.1016/S0012-821X(00)00126-6

Jiang, Z., Li, Y., Zhang, Y., & Xu, K. (2015). Analysis of the Distribution of Onshore Sedimentary Basins and Hydrocarbon Potential in China. *Journal of Fundamentals of Renewable Energy and Applications*, *05*(06). https://doi.org/10.4172/2090-4541.1000191

Lee, K. Y. (1984). *Geology of the Chaidamu Basin, Qinghai Province, Northwest China*. *United States Geological Survey*.

Liu, Z., Zhu, C., Li, S., Xue, J., Gong, Q., Wang, Y., et al. (2017). Geological features and exploration fields of tight oil in the Cenozoic of western Qaidam Basin, NW China. *Shiyou Kantan Yu Kaifa/Petroleum Exploration and Development*, *44*(2), 196–204. https://doi.org/10.11698/PED.2017.02.03

Meade, B. J. (2007). Present-day kinematics at the India-Asia collision zone. *Geology*, *35*(1), 81–84. https://doi.org/10.1130/G22924A.1

Meng, Q.-R., & Fang, X. (2008). Cenozoic tectonic development of the Qaidam Basin in the northeastern Tibetan Plateau. *Geological Society of America*, *444*(01), 1–24. https://doi.org/10.1130/2008.2444(01)

Molnar, P., & Tapponnier, P. (1977). Relation of the tectonics of eastern china to the india-eurasia collision: Application of slip-line field theory to large-scale continental tectonics. *Geology*, *5*(4), 212–216. https://doi.org/10.1130/0091-7613(1977)5<212:ROTTOE>2.0.CO;2

"National Bureau of Statistics." (2016). *China Statistical Yearbook 2016*. https://doi.org/10.1017/CBO9781107415324.004

Ritchie, H., & Roser, M. (2020). Fossil fuels. https://doi.org/10.1016/0306-2619(94)90074-4

Shaw, J. H. (2018). Introduction to Energy Technology: Renewable and Depletable. *Michael J Aziz and Alexander C Johnson*.

Sorin-George, T., & Cătălin, G. (2018). Chinese Economic Pragmatism: The Belt and Road Initiative. *Ovidius University Annals, Economic Sciences Series*, *XVIII*(2), 70–74.

Sun, Y. (2019). *Cenozoic Deformation of the Qaidam Basin, Western China*. Harvard University.

Tapponnier, P., Zhiqin, X., Roger, F., Meyer, B., Arnaud, N., Wittlinger, G., & Jingsui, Y. (2001). Oblique stepwise rise and growth of the tibet plateau. *Science*, *294*(5547), 1671–1677. https://doi.org/10.1126/science.105978

Ullman, D. (2019). When Coal Comes to Paradise. Retrieved from https://foreignpolicy.com/2019/06/09/when-coal-came-to-paradise-china-coal-kenya-lamu-pollution-africa-chinese-industry-bri/

Underwood, M. (2012). China Import Countries. Brookings Institution.

Wang, G. C., Sun, M. Z., Gao, S. F., & Tang, L. (2018). The origin, type and hydrocarbon generation potential of organic matter in a marine-continental transitional facies shale succession (Qaidam Basin, China). *Scientific Reports*, *8*(1), 1–15. https://doi.org/10.1038/s41598-018-25051-1

Wang, Q., & Coward, M. P. (1990). the Chaidam Basin (Nw China): Formation and Hydrocarbon Potential. *Journal of Petroleum Geology*, *13*(1), 93–112. https://doi.org/10.1111/j.1747-5457.1990.tb00255.x

Welte, D. (2002). Petroleum Systems Modeling : A Guidance Tool for the Upstream Petroleum Industry. *ENERGY EXPLORATION & EXPLOITATION*, *20*(5), 401–405.

Wu, L., Xiao, A., Ma, D., Li, H., Xu, B., Shen, Y., & Mao, L. (2014). Cenozoic fault systems in southwest Qaidam Basin, northeastern Tibetan Plateau: Geometry, temporal development, and significance for hydrocarbon accumulation. *AAPG Bulletin*, *98*(6), 1213–1234. https://doi.org/10.1306/11131313087

Yue, Y., Ritts, B. D., Graham, S. A., Wooden, J. L., Gehrels, G. E., & Zhang, Z. (2004). Slowing extrusion tectonics: Lowered estimate of post-Early Miocene slip rate for the Altyn Tagh fault. *Earth and Planetary Science Letters*, *217*(1–2), 111–122. https://doi.org/10.1016/S0012-821X(03)00544-2

Zheng, M., Li, J., Wu, X., Wang, S., Guo, Q., Yu, J., et al. (2018). China's conventional and unconventional natural gas resources: Potential and exploration targets. *Journal of Natural Gas Geoscience*, *3*(6), 295–309. https://doi.org/10.1016/j.jnggs.2018.11.007

Zhuang, G., Hourigan, J. K., Ritts, B. D., & Kent-Corson, M. L. (2011). Cenozoic multiple-phase tectonic evolution of the northern Tibetan Plateau: Constraints from sedimentary records from Qaidam basin, Hexi corridor, and Subei basin, northwest China. *American Journal of Science*, *311*(2), 116–152. https://doi.org/10.2475/02.2011.02

Appendix A – TOC and HI Data

Jurassic Source Rock

Data	Value	Source
Low HI	20	(G. C. Wang et al., 2018)
Median HI	40	(G. C. Wang et al., 2018)
High HI	100	(G. C. Wang et al., 2018)
Low TOC	3	(Lee, 1984)
Median TOC	7	(Lee, 1984)
High TOC	10	(Lee, 1984)

Paleogene Source Rock

Data	Value	Source
Low HI	2	Interpolation
Median HI	2.3	(Liu et al., 2017)
High HI	5	Interpolation
Low TOC	0.32	Interpolation
Median TOC	0.48	(Liu et al., 2017)
High TOC	1.5	Interpolation

Quaternary Source Rock

Data	Value	Source
Low HI	10	(G. C. Wang et al., 2018)
Median HI	20	(G. C. Wang et al., 2018)
High HI	40	(G. C. Wang et al., 2018)
Low TOC	3	(G. C. Wang et al., 2018)
Median TOC	5	(G. C. Wang et al., 2018)
High TOC	7	(G. C. Wang et al., 2018)